Journal of Pharmaceutical Analysis 13 (2023) 111–126

Contents lists available at ScienceDirect

Journal of Pharmaceutical Analysis

journal homepage: www.elsevier.com/locate/jpa

Review paper

Microneedle-based interstitial fluid extraction for drug analysis: Advances, challenges, and prospects

Shuwen Ma [a, 1], Jiaqi Li [a, 1], Lixia Pei [b], Nianping Feng [a, **], Yongtai Zhang [a, *]

[a] Department of Pharmaceutical Sciences, Shanghai University of Traditional Chinese Medicine, Shanghai, 201203, China
[b] Institute of Traditional Chinese Medicine Surgery, Longhua Hospital Affiliated to Shanghai University of Traditional Chinese Medicine, Shanghai, 200032, China

ARTICLE INFO

Article history:
Received 9 October 2022
Received in revised form
28 December 2022
Accepted 31 December 2022
Available online 6 January 2023

Keywords:
Microneedle
Interstitial fluid
Biomarker
Pharmaceutical analysis
Diagnosis

ABSTRACT

Similar to blood, interstitial fluid (ISF) contains exogenous drugs and biomarkers and may therefore substitute blood in drug analysis. However, current ISF extraction techniques require bulky instruments and are both time-consuming and complicated, which has inspired the development of viable alternatives such as those relying on skin or tissue puncturing with microneedles. Currently, microneedles are widely employed for transdermal drug delivery and have been successfully used for ISF extraction by different mechanisms to facilitate subsequent analysis. The integration of microneedles with sensors enables in situ ISF analysis and specific compound monitoring, while the integration of monitoring and delivery functions in wearable devices allows real-time dose modification. Herein, we review the progress in drug analysis based on microneedle-assisted ISF extraction and discuss the related future opportunities and challenges.

1. Introduction

Given the safety risks posed by improper drug dosing, the quantitation and monitoring of ingested pharmaceuticals is a task of high practical significance [1]. Drug testing is frequently performed using blood samples, and the blood concentration range is commonly employed as a dosage guide because of the correlation between blood concentration and treatment outcome [2,3]. This administration method is superior to empirical dosing and allows for timely dose and dosing interval adjustment, thus helping to reduce the incidence of inappropriate dosing-induced adverse effects while improving therapeutic efficacy. However, invasive blood collection poses the risk of infection and is, in some cases, uncomfortable and challenging to carry out, while blood collection, transportation, and handling are time-consuming and expensive processes. These drawbacks have prompted the search for alternative body fluids (e.g., urine, saliva, and tear fluid) as blood substitutes for drug testing, with interstitial fluid (ISF) currently showing the greatest promise [4–7].

ISF contains biomarkers comparable to those found in blood and can therefore be extracted for drug or biomarker analysis to monitor disease conditions and change dosage regimens for customized treatment [7]. However, as current ISF extraction methods are time-consuming and require specialist handling and bulky equipment, reliable and user-friendly ISF extraction techniques have to be developed [8,9].

Acupuncture, a frequently employed traditional Chinese medicine therapy, is an effective method of ISF sampling and can be carried out using many kinds of needles, including filiform and plum-blossom ones [10,11]. In acupuncture, "microneedle" refers to a tiny needle device and (broadly) to any of the nine types of needles. Herein, the term "microneedle" refers to micron-sized structures with sharp needle-like tips and needles with lengths of hundreds of microns [12].

In view of the limited loading capacity of a single needle, several needles are typically placed on a base to create organized arrays for user convenience. In 1998, Henry et al. [13] presented microneedles as a new form of transdermal drug delivery and showed that this approach allows one to greatly enhance transdermal drug permeability.

Microneedles offer the advantages of low production costs and minimally invasive procedures [14,15]. Furthermore, unlike that of injection and blood collection needles regularly used in clinical practice, the administration of microneedles is painless, simple to conduct, and can be performed by patients themselves, which

Peer review under responsibility of Xi'an Jiaotong University.
* Corresponding author.
** Corresponding author.
E-mail addresses: npfeng@shutcm.edu.cn (N. Feng), analysisdrug@126.com (Y. Zhang).
[1] Both authors contributed equally to this work.

https://doi.org/10.1016/j.jpha.2022.12.004

benefits patient compliance [16]. In view of these advantages, microneedles are highly competitive and are frequently employed in cosmetics and transdermal medication delivery [17]. Moreover, recent publications suggest that microneedles can be used for ISF extraction [18]. Regarding real-time monitoring, one study evaluated the concentration of glucose in microneedle-extracted ISF, showing that this approach allows diabetic patients to monitor their blood glucose levels more easily [19]. A patch sensor integrating porous poly(lactic acid) microneedles and an immunochromatographic assay allowed the rapid (within 3 min) detection of severe acute respiratory syndrome coronavirus 2 immunoglobulin G and M antibodies in ISF and thus enabled the rapid diagnosis of Corona Virus Disease 2019 (COVID-19) [20].

This review describes the progress in microneedle-based ISF extraction for drug analysis, with the focus on the combined use of microneedles and sensors for in situ ISF extraction and the subsequent analysis of specific substances [21–23], microneedle-based home monitoring [24–26], and wearable microneedle devices with integrated monitoring and delivery functions [27,28]. Furthermore, we discuss the microneedle-based extraction of plant ISF for target compound monitoring and the potential of this method for the quality evaluation of herbal medicines [29–31].

2. Microneedle types and working principles

Microneedles can be produced by using molding, laser processing, 3D printing, and other methods [32–35]. Silicon, metals, and polymers are frequently used as microneedle materials, with mechanical strength and biocompatibility typically prioritized in material selection [36–38].

The development of processing technologies has enabled the fabrication of many types of microneedles to satisfy diverse requirements, as exemplified by porous and core-shell microneedles [39,40]. Most commonly, microneedles are classified into solid,

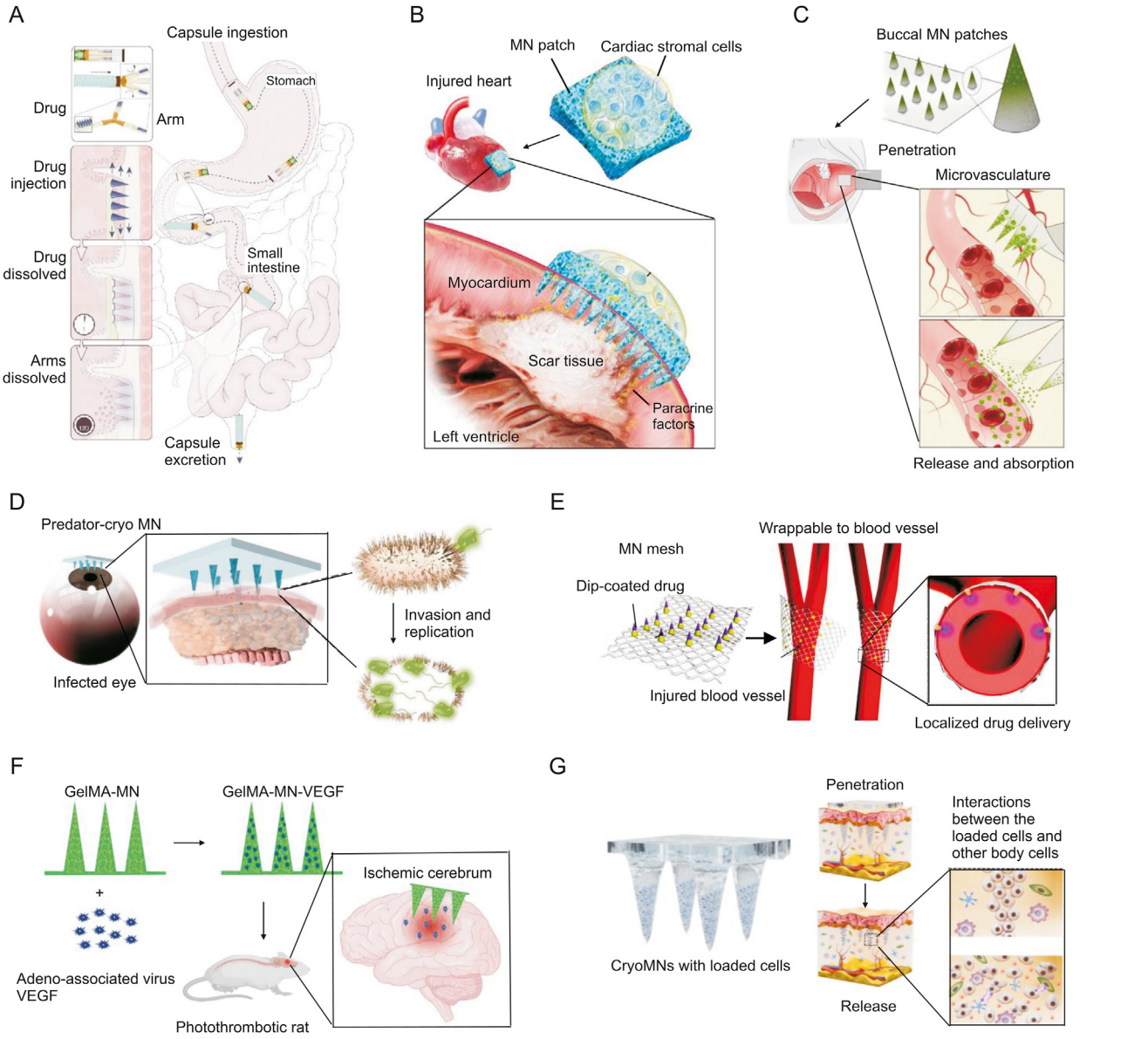

Fig. 1. Microneedle (MN)-assisted drug administration technologies. Microneedle-based delivery of (A) drugs to the intestinal tract [52], (B) cardiac stromal cells to the heart for myocardial infarction treatment [53], (C) active pharmaceutical ingredients to the oral cavity [54], and (D) predatory bacteria to the eye to treat infection [55]. (E) Delivery of drugs to blood vessels by a microneedle mesh [59]. (F) Delivery of an adeno-associated virus expressing human vascular endothelial growth factor (VEGF) to the brain of a photothrombotic rat by gelatin methacryloyl (GelMA)-MNs to promote angiogenesis and functional recovery after stroke [60]. (G) Through-skin drug delivery to cells by microneedles [51]. (Reprint from Refs. [51–55,59,60] with permission.)

hollow, coated, hydrogel, and dissolving types [41–45], but can also be categorized according to other factors such as delivery method, material, and degradability.

Microneedles can deliver various substances (e.g., chemicals, vaccines [46–49], high-energy photons [50], and cells [51]) through diverse biological barriers, which are not limited to the skin and also include the gastrointestinal tract [52], heart [53], oral cavity [54], eyes [55–58], blood vessels [59], and brain tissue [60,61] (Fig. 1) [51–55,59,60].

Microneedles are also used in diagnostics and can be integrated with sensors to realize the direct monitoring of physiological parameters, medications, and biomarkers. Alternatively, microneedles can be used to sample different body fluids and identify and quantify the compounds contained therein.

Fig. 2 illustrates the working principles of different types of microneedles. Solid microneedles pierce the skin to create a microincision that is then used to collect body fluids and deliver actives to the target of action [41]. As their name suggests, coated microneedles feature a surface-coated core. In the case of drug delivery, this coating is often a combination of a drug and a polymer. In the case of drug analysis, the coating resembles a semipermeable membrane and is used to collect bodily fluids [62]. Additionally, coated microneedles can be integrated with sensors for drug and biomarker monitoring and collection [63]. The internal channels of hollow microneedles are employed to deliver medications to tissues or collect fluid from the same [42]. Dissolvable microneedles dissolve after their insertion into tissues, and ISF escapes through the holes formed on the tissue surface [64,65]. The material of hydrogel microneedles has good swelling capabilities and forms a gel after water absorption but does not disintegrate, allowing drug administration or fluid aspiration [66].

Particular types of microneedles are preferred for both delivery and diagnostic purposes, as different microneedles absorb and transport chemicals according to distinct principles. Notably, although microneedles have been extensively used on humans or animals such as mice and pigs, they have not been widely applied to plants.

3. Use of microneedles for drug analysis

3.1. Drug analysis and monitoring

The advent of modern medicine and the accompanying enhancement of living standards have made people more mindful of their health and inspired the development of precision therapy [67].

The therapeutic effect of a given medicine is affected by its pharmacokinetic and metabolic characteristics. As these characteristics can greatly vary between individuals, drug administration therapy should be tailored on an individual basis. Such individualized drug administration can boost therapeutic effects and clinical efficacy while lowering the probability of adverse side effects (e.g., toxicity and drug resistance) and enhancing medication safety. For instance, inadequate antibiotic dosing may cause resistance. One requirement for achieving personalization is the necessity to monitor the dose of the administered drug in the patient's body.

Therapeutic drug monitoring (TDM) is the process of measuring drug plasma concentration, comparing it to the target concentration, and applying pharmacokinetic principles to guide dosing based on the obtained results. To date, TDM has been used to guide the administration of many medications, such as β-lactam antibiotics, antiepileptics, and infliximab, and therefore has substantial implications for the treatment of numerous disorders [68–71] and is viewed as a crucial auxiliary for achieving individualized medication delivery [72].

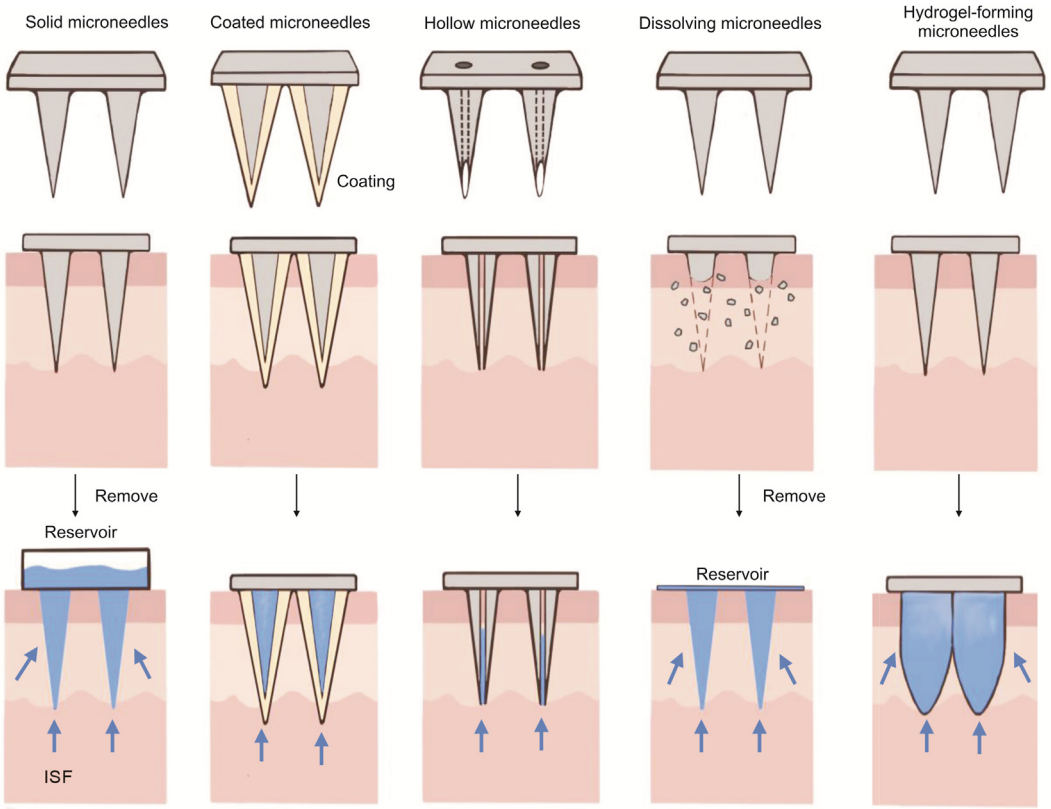

Fig. 2. Structures of different microneedles and schematic diagram of the related extraction mechanisms.

3.2. Suitability of ISF for drug analysis

Although the blood is commonly used for medical diagnostic analysis, it has several drawbacks. For example, blood sampling necessitates venipuncture by medical professionals, which is especially challenging in newborns, babies, and patients with frail veins, and may result in dread and anxiety [73]. In some nations and places, blood collection needles are reused without sterilization, which increases the danger of disease transmission [74]. Blood drawing can pose health risks to some patients. In some cases, the test is performed on plasma or serum, requiring pre-processing of the blood sample by centrifugation, etc. In such cases, many milliliters of blood are taken from the patient, while only a few microliters of the sample are actually used for the test, resulting in sample wastage [75]. Addition of anticoagulant to the collected blood, followed by centrifugation, is important to obtain plasma, which is devoid of blood cells. When no anticoagulant is added, clotting factors in the blood initiate the clotting pathway, causing the conversion of soluble fibrinogen to insoluble fibrin,and resulting in division of the blood into clots and serum [76] (Fig. 3A) [42]. Incorrect use of anticoagulants, leaving the blood sample for too long, improper handling during blood collection, or ingestion of some medications will cause the blood to clot and the test results will no longer be accurate, requiring resampling [77]. In view of the above, alternative fluids for testing are highly sought after.

ISF is distributed between cells and is the medium for the exchange of substances between blood and tissue cells [78]. Fig. 3B illustrates the body fluid circulation process: water in the digestive tract is absorbed into the capillaries, and at the arterial end of the capillaries, water and small molecules (such as glucose, amino acids, urea, sodium, chloride, electrolytes, and fat-soluble substances) in the plasma, except large protein molecules, can filter through the capillary wall and enter the intercellular space by diffusion to form ISF; at the venous end of the capillaries, most ISF components can be returned to the blood while a few leak into the capillary lymphatic vessels, and the lymphatic fluid enters the vessels of the left and right subclavian veins [79,80]. In other words, ISF is formed from blood plasma and returns to blood plasma, completing the exchange of substances between blood and ISF.

Moreover, there is a correlation between ISF and the concentration of some biomarkers in the blood. As shown in Fig. 3C, the composition and content of ions in ISF and blood are similar under physiological conditions [81]. Proteomic analysis comparison of ISF with plasma and serum was performed in rats, and almost 100% of the 2855 proteins identified in blood-derived samples were also detected in ISF, with the same qualitative analysis results but different quantitative results (Fig. 3D) [42]. Metabolomic assays using healthy human volunteers as samples showed that the number of metabolites specific to plasma was limited; most

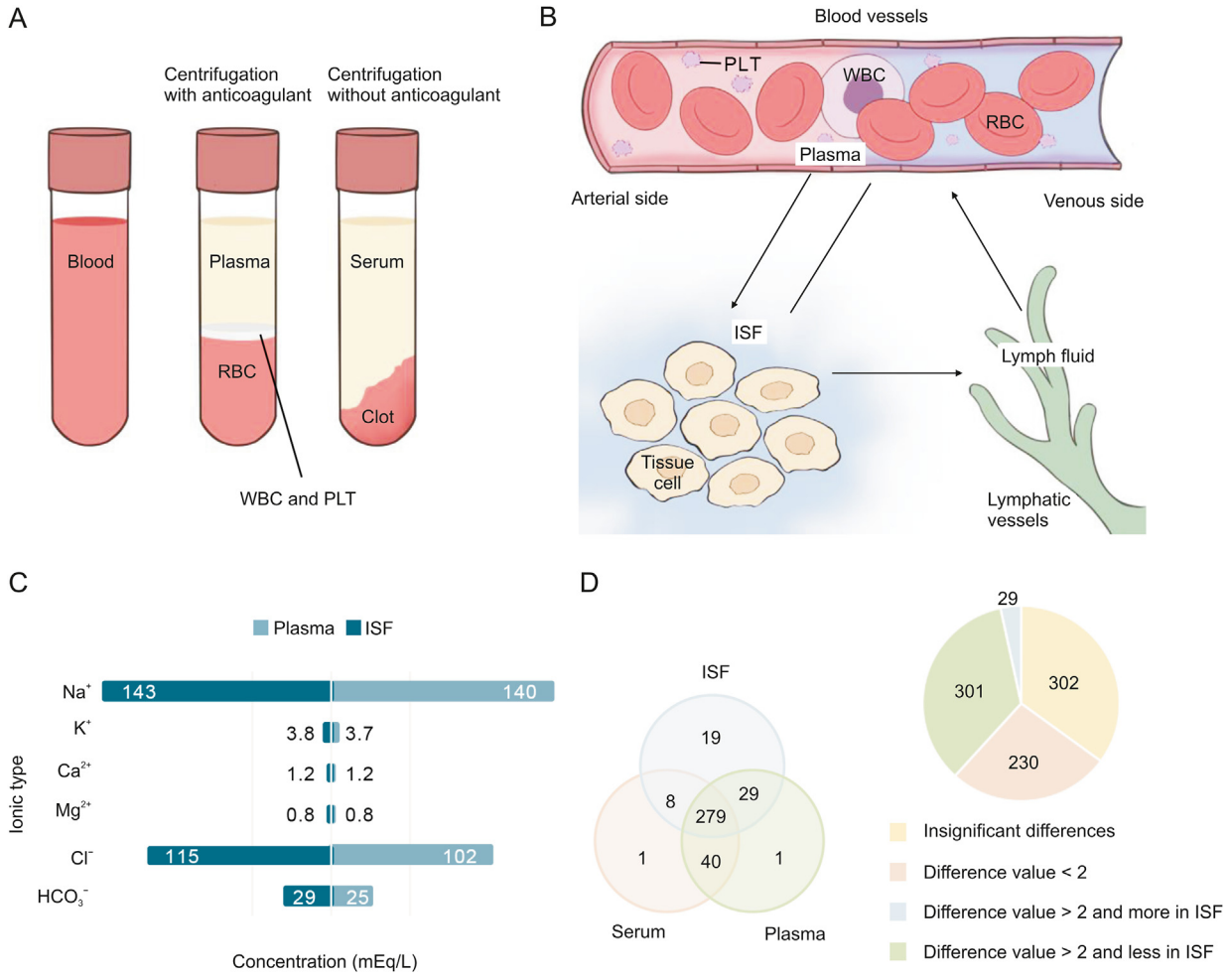

Fig. 3. Comparison of component testing in interstitial fluid (ISF) and blood. (A) Separation of plasma and serum from blood. (B) Circulation of plasma, ISF, and lymph fluid, focusing on the source and destination of ISF. (C) The composition and concentration of ions in ISF and blood. (D) Results of proteomic analysis of ISF, plasma, and serum [42]. RBC: red blood cell; WBC: white blood cell; PLT: platelet. (Reprint from Ref. [42] with permission.)

Table 1
Metabolites that are more abundant in interstitial fluid (ISF) compared to plasma and their effects.

Name	Role of the metabolite	Uniqueness	Refs.
Urocanic acid	Have immunosuppressive effects and may play a detrimental role in photocarcinogenesis	Unique to ISF	[82,83]
Spermidine	Associated with anti-aging mechanisms		[82,84]
Phosphocreatinine and creatine	A potential biomarker of mitochondrial diseases		[82,85]
Hypoxanthine and inosine	Biomarkers for cardiac ischemia		[82,86]
Glycerophosphocholine	Biomarker for breast cancer		[82,87]
3-methylsulfinylpropyl isothiocyanate	As a compound with potent anti-inflammatory effects	Unique to ISF	[82,88]

substances were detected qualitatively in both plasma and ISF; and several metabolites, such as homocysteine and betaine, were positively correlated between ISF and plasma, which suggests that their levels in ISF may reflect those in the blood [82]. In addition, there are substances that are specifically found in ISF or have a higher concentration in ISF than that in plasma, and Table 1 [82–88] shows these substances and their effects. Their higher ISF levels can facilitate detection, and there are unique biomarkers in ISF that are not found in the blood, suggesting that sampling ISF may be superior to blood testing for diagnosing certain diseases.

After absorption into the blood, drugs bind to plasma proteins to varying degrees. Bound drugs have no pharmacological activity and cannot easily pass through the vascular wall, while free drugs that are distributed in blood, tissues, and intracellular fluid have pharmacological activity. The lower protein content in the ISF compared to that in blood facilitates the collection of drugs in active form. The extent of drug binding to plasma proteins is an important factor affecting the distribution of drugs in vivo. That is, drugs with low blood protein-binding ability show greater translocation to the ISF. A study used rabbits as study subjects to determine the pharmacokinetics of several drugs that are often monitored clinically, antibiotics (vancomycin and gentamicin), immunosuppressants (tacrolimus, cyclosporine and mycophenolate), anticonvulsants (valproic acid, phenobarbital, and phenytoin sodium), chemotherapeutic drugs (carboplatin, cisplatin, and methotrexate), and other drugs (theophylline and digoxin), in the blood and ISF, comparing various parameters, such as c_{max}, t_{max}, and area under the curve, as the basis to determine the suitability of drugs for ISF monitoring instead of blood monitoring; vancomycin was found to be suitable for ISF monitoring [89]. Fig. 4 shows the process of selecting ISF instead of blood for drug monitoring with examples in the form of a decision tree.

In summary, for the various biomarkers and drugs with positive correlation between their ISF and blood concentrations, the absence of blood cells in ISF reduces sample pre-treatment by centrifugation to remove blood cells. The lower variety and number of clotting factors in ISF do not induce clotting like those in the blood and can be monitored continuously. Finally, the lower protein content in ISF compared to that in the blood facilitates the collection of drugs in their active form, thus making ISF sampling preferable to blood testing for diagnosis.

3.3. ISF extraction methods

As ISF cannot be released or expelled from the body, it must be collected through physiological barriers such as the skin [90]. In the past, microdialysis and suction blisters were frequently used to extract and collect ISF from the skin and tissues [91–93]. These methods require specialized handling and instruments while exhibiting the additional drawbacks of small sampling volume and time-consuming nature; in addition, the corresponding sampling process results in discomfort and/or pain and may cause scarring [94–96]. The above constraints limit the utility of ISF for drug analysis and diagnosis.

Microneedles enable rapid and easy ISF extraction and have been used to collect ISF via the skin. Specifically, microneedles typically penetrate the stratum corneum of the epidermis while avoiding nerve fibers and blood vessels located in the dermis [97]. In comparison to other techniques, microneedle-based ISF extraction is minimally invasive, safe, and painless, featuring the additional benefits of easy-to-use equipment and operation simplicity and thus drawing much attention in the field of drug detection. Moreover, microneedles can be used for biological fluid collection and drug monitoring, including the collection of blood and lymphatic fluid [23,36,98].

4. Microneedle-based ISF extraction for drug analysis

4.1. Microneedle-based ISF sampling

Different microneedles absorb ISF in different ways. For instance, the material of hydrogel microneedles swells to allow ISF to diffuse into the same. This diffusion slows down with increasing amounts of retrieved ISF, which is constrained by microneedle size and swelling capacity. Hollow microneedles aspirate ISF by suction under capillary action [25]; however, when using this technique, one should avoid congestion and be mindful of possible microneedle breakage [99].

Researchers have fully utilized the aforementioned microneedle extraction techniques while intentionally using some external forces to extract more ISF faster. In an exemplary work, a microneedle patch was prepared by mixing an osmotic agent with a hydrogel to provide osmotic pressure during extraction (Fig. 5A), and the accelerated extraction rate allowed for the extraction of 7.90 μL of ISF from isolated pig skin and 3.82 μL of ISF from isolated mouse skin in just 3 min [100]. Similarly, sorbitol hydrogel-forming microneedles were designed to accelerate extraction [101]. Microneedles acting on the skin form micropores, and ISF can be extracted through these micropores using a vacuum pump as a convective driving force [102]. However, in view of the need for specialist training, the use of specialized equipment, and the possibility of the sampled ISF being contaminated with blood, this method is not well suited for general clinical application.

The microneedle material affects the ISF extraction volume and rate. When hydrogel microneedles are used for ISF extraction, the choice of material with full consideration of mechanical and swelling properties is particularly crucial. Previously, a methacrylated hyaluronic acid microneedle patch (Fig. 5B) was reported to extract ~2.3 μL of ISF in 10 min [103]. In recent years, gelatin methacrylate (GelMA) microneedle patches, sponge-forming poly(vinyl acetal) microneedle patches, cross-linked GelMA microneedle patches, and graphene oxide-GelMA microneedles have been fabricated and used for ISF extraction [104–107]. Table 2 [103–107] compares the ISF extraction performances of microneedles composed of various materials.

When punctured by microneedles during ISF extraction, the skin experiences small deformations, and the force applied to the microneedle fluctuates, which may affect the extraction effect.

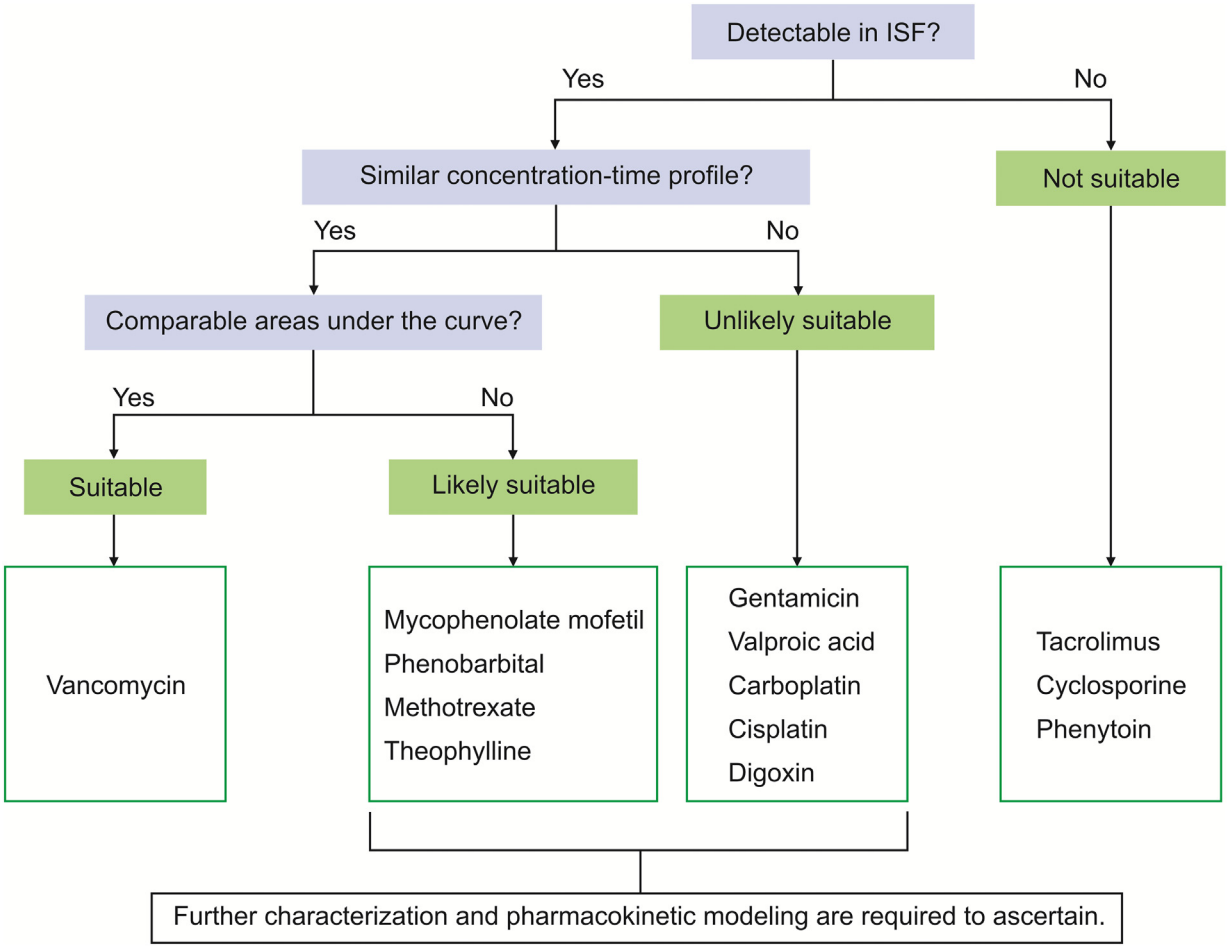

Fig. 4. Decision tree diagram to determine the feasibility of using interstitial fluid (ISF) instead of blood for drug monitoring.

Precision punctures are much more important. As illustrated in Fig. 5C [108], a bee stinger-inspired bionic rotating microneedle allowed the maximum penetration force to be lowered by 45.7% and the rate of force decay to be increased 2.73-fold. This design decreased skin resistance and enabled more precise positioning during puncture.

Many works have focused on enhancing ISF collection following microneedle penetration. For example, two strips of filter paper were attached to both sides of the microneedle base and used to absorb the effluent ISF following microneedle insertion into the skin (Fig. 5D) [109,110], which allowed ~4 μL of ISF to be collected in 1 min. Tran et al. [111] placed ultrafine nanoneedles on a microneedle array holder and attached each needle to a 1–5 μL calibrated pipette capillary. Once the constructed microneedle array was introduced into the skin, ISF was collected into the capillary (Fig. 5E) [111], and 10 μL of ISF was collected within 30 min [42,111].

The above procedures require the creation of micropores in the skin by microneedles to extract ISF, which is then used for in vitro analysis. Significant progress has been made in increasing the ISF extraction volume and decreasing the extraction time through appropriate measures with the aid of external forces, proper material selection, and collection scheme optimization. However, as the extracted ISF must be transferred to another analytical instrument, it still takes a long time to obtain the final analytical results, and sample stability may be insufficient. Additionally, the number of operational processes increases the probability of errors.

4.2. Microneedle and sensor combination for in situ extraction and monitoring

To overcome the disadvantages of separate microneedle sampling and sample analysis, microneedles can be integrated with sensors to achieve in situ real-time drug and biomarker monitoring in ISF.

4.2.1. In vivo drug monitoring

Rawson et al. [112] created a β-lactamase biosensor composed of solid microneedles coupled with an electrode sensor and a β-lactamase layer. In this biosensor, phenoxymethylpenicillin (an antibiotic) reacts with β-lactamase to produce protons and thus reduce the pH of the ISF and induce a phenoxymethylpenicillin concentration-dependent potential shift, which is detected by the electrode sensor and used for antibiotic concentration monitoring.

In accordance with the aforementioned theory, dedicated sensors were created to track penicillin (a β-lactam antibiotic), catecholamines, levodopa, morphine, and fentanyl in ISF [14,113–115], with the obtained results presented in Table 3 [14,112–115] and Fig. 6 [112,114,115].

The integration of microneedles and sensors enables the continuous monitoring of drug concentration; however, the scope and quantities of effectively monitored drugs are rather limited, and sensor anti-interference ability and rapid response capability need to be further examined. In the future, smaller microneedle

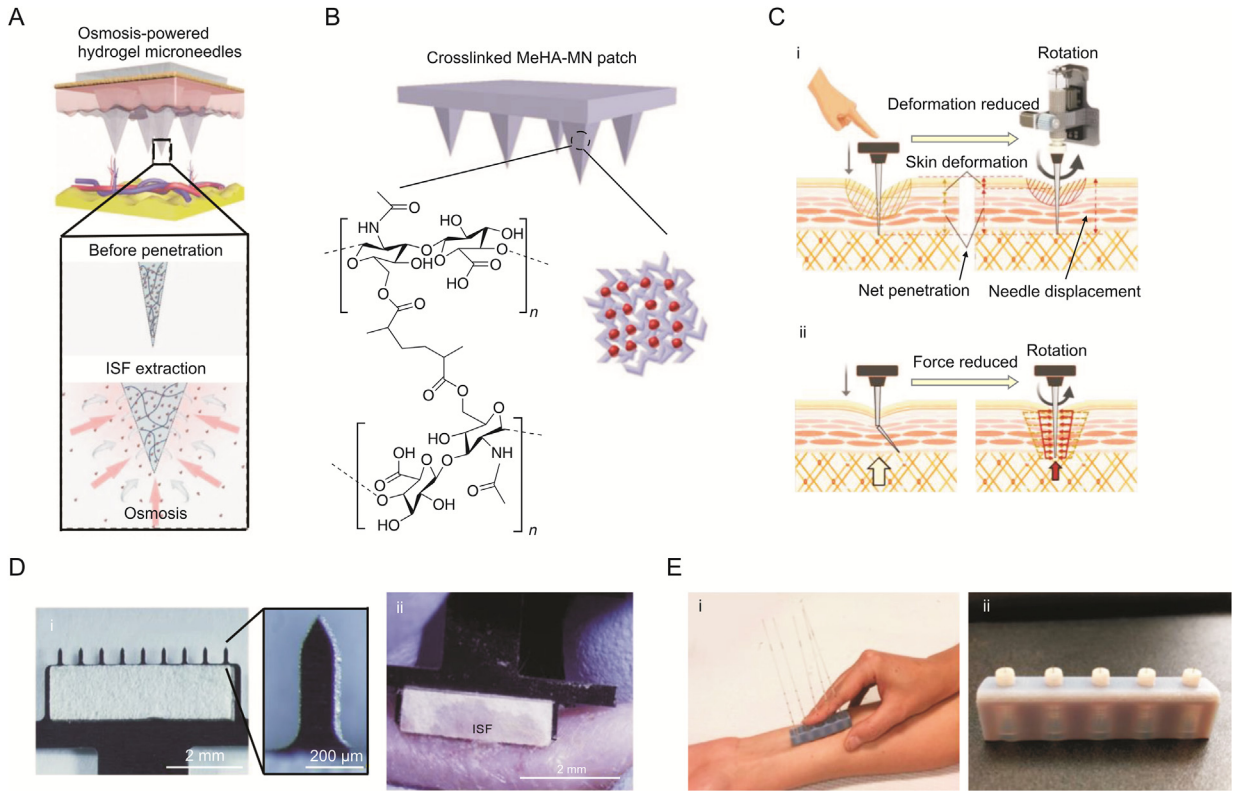

Fig. 5. Improvement of the interstitial fluid (ISF) extraction performance of microneedles through the use of external forces, rational selection of materials, and collection scheme optimization. (A) Hydrogel microneedle with osmotic agent [100]. (B) Methacrylated hyaluronic acid (MeHA)-microneedle (MN) patch with optimized sampling volume and sampling time [103]. (C) Schematic diagram of rotating microneedle (direct manual vertical insertion of microneedles results in a greater degree of skin deformation and lower net penetration compared to rotary microneedle insertion (i); in view of the uncertainty of the discontinuous force during manual vertical insertion, microneedles may break or bend. Microneedle rotation attenuates the sidewall forces acting on the needle and thereby reduces axial friction (ii).) [108]. (D) Filter paper strips attached to both sides of the microneedle base for ISF collection (microneedle extends from the back of the patch, and rectangular filter paper strips are stuck on both sides (i); the microneedle patch is applied to the skin, and ISF flows out of the skin through the produced micropores and is collected on filter paper (ii).) [109,110]. (E) Microneedle device used for ISF collection (the microneedle device has a capillary attached to the needle and acts on the forearm to collect ISF (i); five ultrafine nanoneedles assembled on a 3D-printed support (ii).) [111]. (Reprint from Refs. [100,103,108–111] with permission.)

arrays should be created by reducing the number of electrodes and using biocompatible sensor materials to increase in vivo stability.

4.2.2. Biomarker monitoring

Biomarker monitoring based on the combination of microneedles and sensors has drawn much attention in the case of glucose. Microneedles are frequently grafted with glucose oxidase, which reacts with glucose to induce changes that can be observed by sensors. A hollow silica microneedle array achieved an extraction rate of 1 μL/s [99]. Surface-enhanced Raman spectroscopy was paired with poly(methylmethacrylate) microneedle-based extraction to construct glucose biosensors; specifically, silver-plated microneedle arrays surface-doped with 1-decanethiol permitted rapid measurements in the range of 0–20 mM and allowed for good skin recovery within 10 min after measurement [116]. Despite significant advancements in microneedle glucose sensors, long-term stability and continuous monitoring remain unresolved issues. In terms of stability, a recent work presented an array of 55 hollow microneedles integrated with a glucose biosensor covered with a redox mediator bilayer consisting of Prussian blue and iron-nickel hexacyanoferrate, revealing that this design boosts the long-term stability of readings [117]. The array was attached to a syringe using a microfluidic tube to make ISF extraction faster than glucose diffusion. For continuous monitoring, researchers created a patch-type supercapacitor capable of self-charging under the action of electrons provided by glucose oxidation. In this system, charging began when a potential difference was established at the supercapacitor electrodes. This setup eliminated the need for batteries by providing a constant power supply. The power

Table 2
Interstitial fluid (ISF) extraction performances of microneedles composed of different materials.

Microneedle material	Sampling volume (μL)	Time (min)	Sample object	Refs.
Methacrylate	2.3 ± 0.4	10	Mice	[103]
GelMA	2.5	10	Rats	[104]
Poly(vinyl acetal)	1.6	1	Rats	[105]
c-GelMA	3.5 ± 0.1	30	Agarose gel system model	[106]
Graphene oxide-GelMA	21.34	30	Human skin	[107]

GelMA: gelatin methacrylate; c-GelMA: cross-linked GelMA.

Table 3
Overview of microneedle sensors used for drug monitoring.

Microneedle type	Sensor	Monitored substance	Object	Result	Refs.
Solid	β-lactamase biosensor	Penicillin	Healthy volunteers	Preliminary data suggested that this system tracked blood and microdialysis levels.	[14]
Solid	β-lactamase biosensor	Phenoxymethylpenicillin	Healthy volunteers	First microneedle-biosensor system for antibiotic monitoring. The results were in line with the current common use of microdialysis. However, 16% of the data could not be used for follow-up analysis.	[112]
Solid	Electrochemical sensors	Catecholamines	Artificial interstitial fluid (ISF) and skin models	The device was biocompatible and had high sensitivity and stability for the detection of three structurally similar catecholamines. However, the observed signals were indistinguishable.	[113]
Solid	Biosensor	Levodopa	Skin model	The dynamic concentration monitoring of levodopa in patients with Parkinson's disease is important for reducing the occurrence of complications.	[114]
Hollow	Electrochemical sensors	Opioids (morphine, fentanyl)	Skin model	The microneedle sensor was highly sensitive and could be used to differentiate between opioid overdose and nerve agent poisoning for immediate medical treatment. However, it was not a universal opioid detector.	[115]

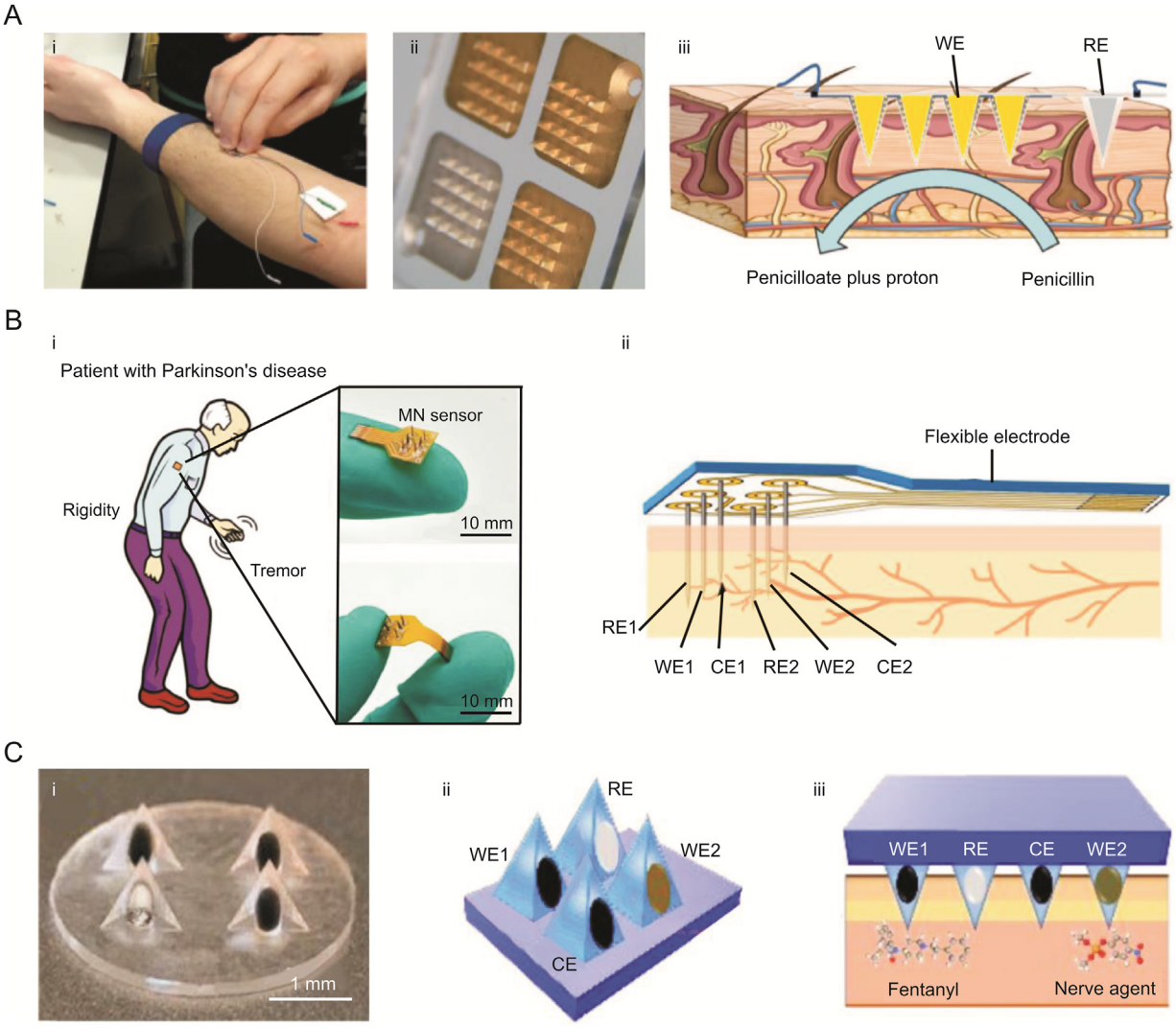

Fig. 6. Microneedle (MN) biosensors for drug monitoring. (A) Schematic design and use of microneedle biosensors (pressure is applied to the microneedle biosensor in the forearm (i); microneedle array diagram (ii); schematic diagram of microneedle array penetrating the dermis (iii).) [112]. (B) Microneedle sensor-based levodopa monitoring (schematic diagram of minimally invasive levodopa sensor for dynamic monitoring of levodopa in patients with Parkinson's disease (i); schematic diagram of subcutaneous microneedle array implantation (ii).) [114]. (C) Hollow microneedle-based electrochemical sensor for opioid monitoring (optical image of microneedle sensor array (i); schematic diagram of microneedle sensor array (ii); schematic diagram of microneedle sensor array simultaneously detecting opioids and nerve agents (iii).) [115]. RE: reference electrode; WE: working electrode; CE: counter electrode. (Reprint from Refs. [112,114,115] with permission.)

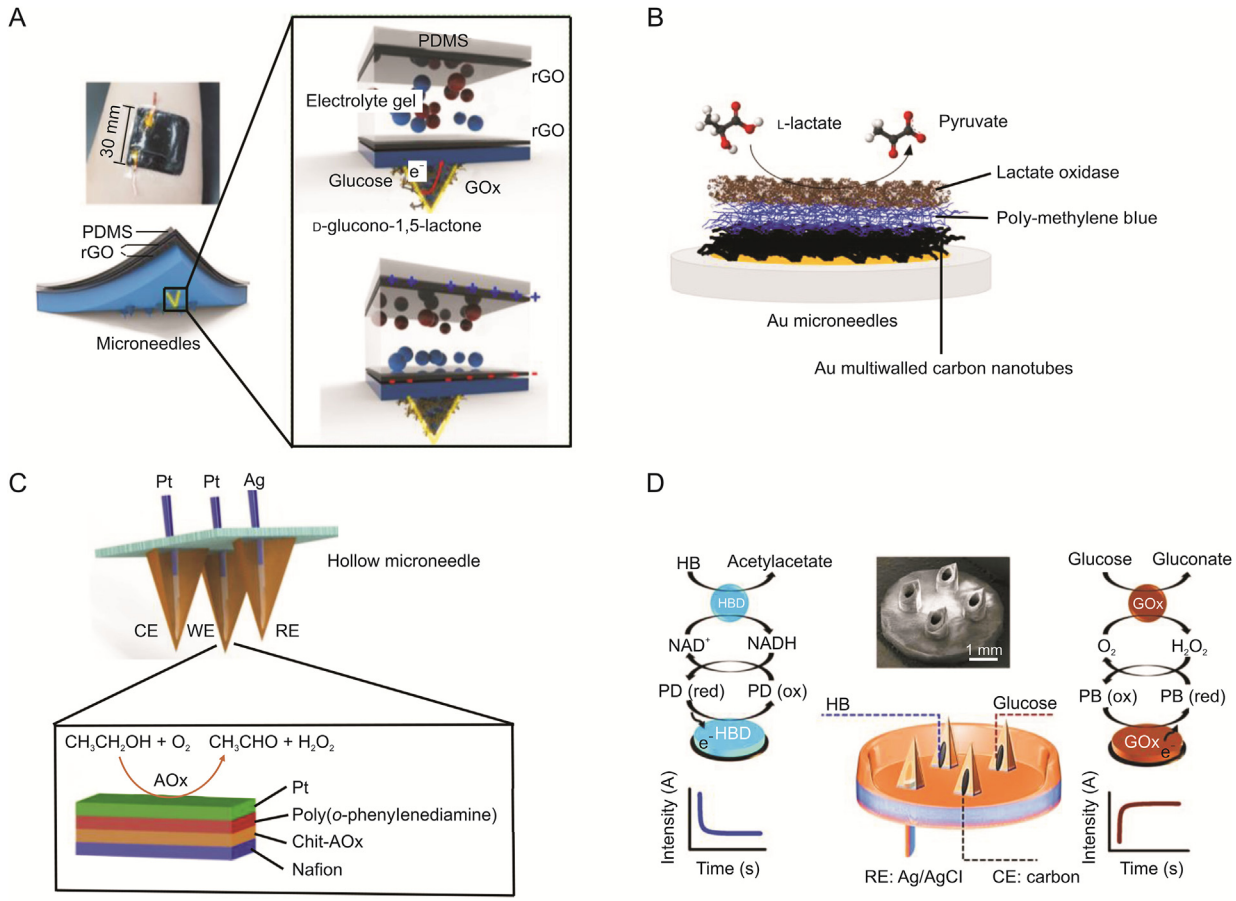

Fig. 7. Microneedle biosensors for biomarker monitoring. (A) Structure and working principle of a self-charging microneedle patch for glucose biosensing [118]. (B) Schematic diagram of a microneedle surface-modified electrode for lactate monitoring [119]. (C) Hollow microneedle biosensor with integrated platinum and silver wires for alcohol monitoring [120]. (D) Microneedle sensor for the simultaneous monitoring of ketone bodies and glucose ([22]). PDMS: poly(dimethylsiloxane); GOx: glucose oxidase; rGO: reduced graphene oxide; CE: counter electrode; WE: working electrode; RE: reference electrode; AOx: alcohol oxidase; Chit-AOx: immobilization of AOx in an intermediate chitosan layer; HB: β-hydroxybutyrate; HBD: HB dehydrogenase; PD: phenanthroline dione; PB: Prussian blue. (Reprint from Refs. [22,118–120] with permission.)

density of self-powered solid-state supercapacitors (SPSCs) in an 11 mM glucose solution reached 0.62 mW/cm^2. The voltage change of SPSCs charged by glucose oxidation was used to determine blood glucose concentration following the same logic as that applied to self-powered biosensors, in which case the output power was proportional to reactant concentration (Fig. 7A) [118].

Other commonly monitored substances besides glucose include lactic acid and alcohol. To monitor lactate, Bollella et al. (Fig. 7B) [119] electrodeposited lactate oxidase, poly(methylene blue), and gold-coated multiwalled carbon nanotubes onto the gold-coated surface of microneedles, achieving high sensitivity and a low detection limit. A hollow microneedle surface was paired with multiple poly(o-phenylenediamine)/chitosan layer-alcohol oxidase/Nafion coatings and integrated Pt and Ag leads within the microneedle aperture to produce a microneedle triple electrode system for efficient subcutaneous alcohol monitoring in an ex vivo mouse skin model (Fig. 7C) [120].

A wearable clustered regularly interspaced short palindromic repeats-associated 9 (Cas9) microneedle patch integrating a reverse ion introduction module and a biosensor allowed for the real-time in vivo monitoring of the Epstein-Barr virus, sepsis, and kidney transplant cell free DNA (cfDNA) for 10 days while maintaining 60% fetal bovine serum resistance [121]. This system may be used for the early detection and real-time monitoring of diseases related to cfDNA.

Ion monitoring is crucial for determining health state, as electrolyte imbalance is linked to numerous ailments. Solid microneedles (length = 1000 μm, tip angle = 45°, tip thickness = 15 μm, base = 435 μm) were modified with different coatings and polymer films to fabricate working and reference electrodes and inserted into the skin to realize the monitoring of potassium ions in ISF by potential sensing [122]. The patch could be used for more than 24 h without any side effects on skin cells, and the in vivo applicability of this design was demonstrated by the measurement of potassium concentrations in chickens and pigs. However, parameters such as the strength of membrane adhesion to the microneedle have to be further studied. A platform consisting of a solid polystyrene microneedle sensor, a field-effect transistor, and an extended gate was successfully used to monitor sodium ions in ISF based on the conversion of sodium ion concentration into an electrical signal by the field-effect transistor [21]. The sensor exhibited high sensitivity, a low detection limit, good biocompatibility, and high mechanical stability. Thus, microneedle electrodes modified by chemical doping, selective membranes, antibodies, and enzymes can be used to develop sensors for the detection of multiple biomarkers.

The integration approach enables the simultaneous monitoring of several biomarkers by a single microneedle array. Hollow microneedles with an appropriate electrode material at the tip were modified with β-hydroxybutyrate dehydrogenase for the electrochemical monitoring of β-hydroxybutyrate (HB) via an

Table 4
Overview of microneedle sensors used for biomarker monitoring.

Microneedle type	Sensor	Monitored substance	Object	Result	Refs.
Solid	Biosensor	Sodium	ISF	Rapid real-time detection of sodium ions was achieved.	[21]
Hollow	Potentiometric sensor	Ketone bodies	Skin model	The sensor simultaneously detected ketone bodies and glucose, holding promise for automated diabetes management.	[22]
Hollow	Biosensor	Glucose	ISF	The sensor was used for the field monitoring of relevant parameters and enabled painless glucose quantitation in ISF.	[99]
Hollow	Electrochemical biosensor	Glucose	ISF	The sensor was more stable than existing microneedle-based glucose monitoring devices.	[117]
Solid	Biosensor	Glucose	Skin model	The design enabled a continuous power supply, thus allowing signals to be recorded in the absence of batteries. Blood glucose levels were monitored in real time without the need for additional bulky energy storage devices.	[118]
Solid	Biosensor	Lactate	ISF	The sensor contributed to the development of a real-time monitoring device for use in sports medicine and clinical care.	[119]
Hollow	Biosensor	Alcohol	Mice	The sensor contributed to continuous non-invasive alcohol monitoring.	[120]
Solid	Biosensor	cfDNA	Skin chip	The wearable microneedle patch enabled the continuous in vivo monitoring of cfDNA, showing good electrochemical performance and stability.	[121]
Solid	Potentiometric sensor	Potassium	Chicken and pig	The sensor featured a low response time and good selectivity and repeatability, aiding the preventive diagnosis and personalized treatment of electrolyte imbalance disorders.	[122]

ISF: interstitial fluid; cfDNA: cell free DNA.

enzymatic reaction, and the simultaneous detection of HB/glucose or HB/lactate could be conducted on the microneedle array following integration (Fig. 7D) [22]. HB is the main biomarker of ketone body formation and is therefore important for the monitoring of diabetic ketoacidosis.

Table 4 [21,22,99,117–122] introduces microneedle sensors used for biomarker monitoring. Compared with other continuous monitoring devices, microneedle arrays are smaller, painless, less irritating and traumatic to the skin, and less likely to cause local infection and bleeding. Although the integration of microneedles and sensors enables in situ real-time drug monitoring, individual biosensors are required for each drug. Hence, the creation of drug-specific sensors is crucial for expanding the scope of monitored drugs. Moreover, some technical difficulties need to be overcome. Regarding monitoring accuracy, the sensor should be sufficiently sensitive, and calibration during operation should be precise. The fact that most substances are present in ISF in low amounts inspires further research on decreasing sensor detection limits. Biocompatible materials should be researched to increase the in vivo stability of sensors, as the deployment of some sensors is accompanied by the insertion of microneedles into the body. Material safety should also be considered. Finally, smaller and more transportable components are required for system integration.

4.3. Microneedle-based home diagnosis

In the context of the COVID-19 pandemic, microneedle-assisted drug monitoring holds great promise. Microneedle systems have been used for COVID-19 vaccination, and the microneedle storage of vaccines has been shown to reduce the dependence on the cold chain and lower transportation costs. Moreover, the pattern of the microneedle array arrangement is retained in the skin using fluorescent dyes, which enables the recording of and rapid access to vaccination information without the use of storage devices and thus saves labor and material resources [123,124]. Furthermore, in view of the operational policies such as those relating to isolation, many people have difficulty accessing hospitals. As many patients with cancer or other chronic diseases require long-term monitoring of the relevant biomarkers for treatment optimization, the research and development of microneedle-based home testing devices is essential.

4.3.1. Smartphone-based systems

A subcutaneous device for in vivo glucose sensing was created using a smartphone application and interfaced with a touchscreen glucose sensor and an easy-to-use wireless chemical detector (Fig. 8A) [125]. The glucose sensor had a radius of 14 mm and a thickness of 2.7 mm and carried stainless steel microneedles (25 solid microneedles with an average height, tip diameter, and base diameter of ~2.2 mm, 30 μm, and 400 μm, respectively). In vivo tests on diabetic rats revealed that this device is affordable and simple to use, and can be operated by non-professional patients. A significant benefit of smartphone usage is the visual presentation of data, which allows users to access the concentrations of the monitored substances in real time. Data synchronization also facilitates data collection and interpretation.

4.3.2. Lateral flow cassette-based systems

The primary components of the employed lateral flow cassette (Fig. 8B) [26] were a sample pad, conjugated pad, glass fiber detection pad, and absorption pad, which were successively assembled on a plastic backing plate. The hydrogel microneedle was filled with sodium polyacrylate as an absorbent to enhance swelling and increase the water retention capacity, and the desired amount of ISF could be extracted in 5 min. ISF flowed onto the sample pad, and the T1 line progressively changed color with increasing concentration of cystatin C. When this concentration exceeded the threshold value, the T2 line appeared, and the detection process took only 15 min. Controlled trials demonstrated the high selectivity and specificity of this system [26]. The lateral flow cassette-microneedle system could be used anywhere at any time, and the results could be easily read with the naked eye. However, this method did not allow precise analyte quantitation.

4.3.3. Colorimetric detection-based systems

Hollow microneedles fabricated using conventional photolithography and poly(ethylene glycol) diacrylate were combined with glucose test paper, and the required ISF amount could be collected in 5 min. ISF was transported to the analysis area of the test paper by capillary action provided by the porous structure of the paper substrate, which offered a significant surface area for macromolecule immobilization. After the microneedle penetrated the skin, ISF was extracted to the top of the reaction layer of the

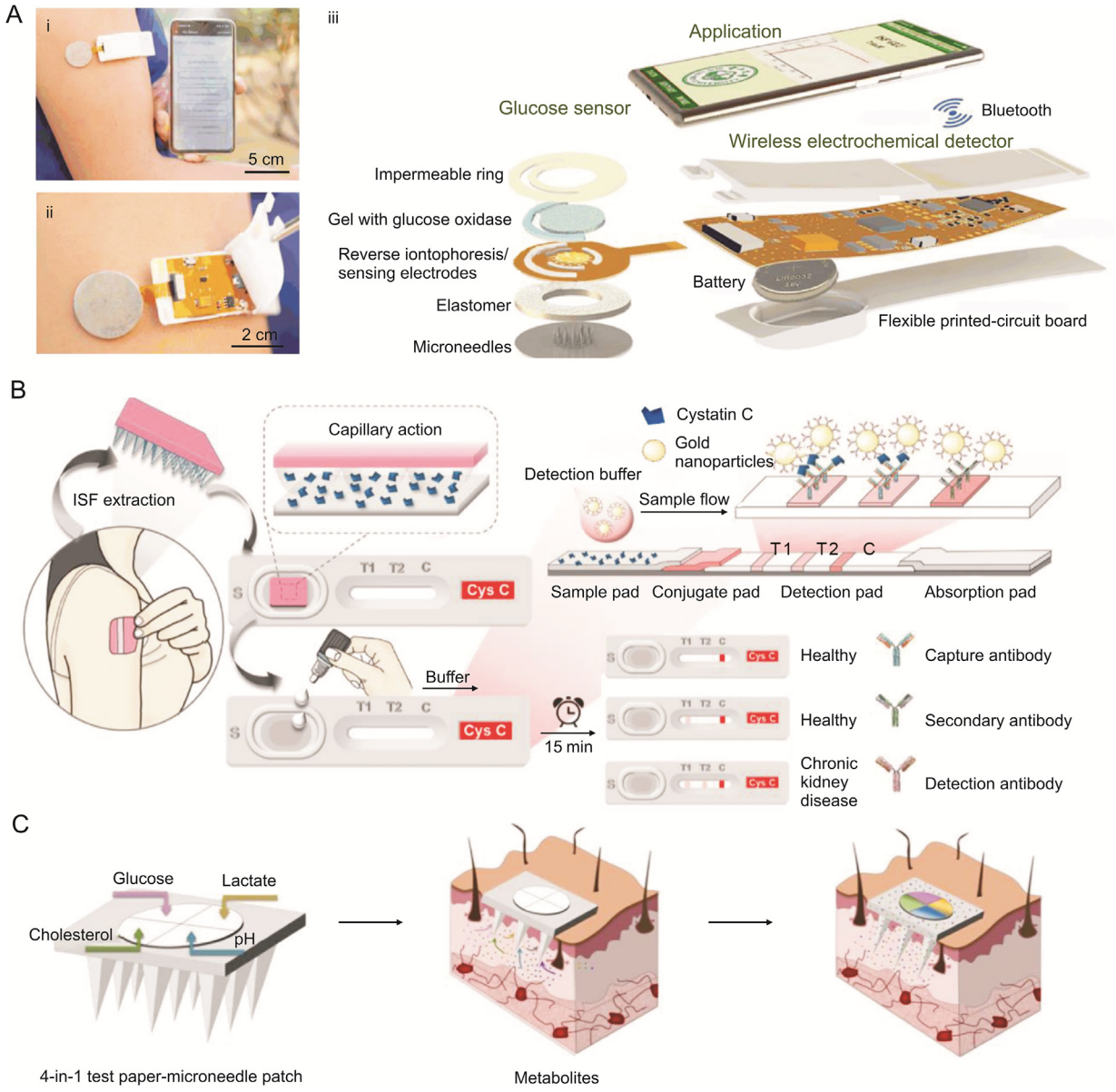

Fig. 8. Microneedle-based home diagnosis. (A) Microneedle combined with a smartphone for glucose monitoring (smartphone-based glucose electrochemical detection platform (GEDP) (i); wireless chemical detector connected to a touch-type glucose sensor for electrochemical glucose detection (ii); schematic diagram of a smartphone-based GEDP consisting of a touch-sensitive glucose sensor, radio chemical detector, and smartphone application (iii).) [125]. (B) Microneedle patch integrated with a lateral flow cassette for the home testing of chronic kidney disease [26]. (C) Diagram of the application process of a four-in-one test paper microneedle patch [24]. T1: test 1; T2: test 2; C: control; Cys C: cystatin C. (Reprint from Refs. [24,26,125] with permission.)

glucose paper, where the glucose was oxidized to produce H_2O_2 and gluconic acid. Under the influence of H_2O_2, the color of the paper turned yellow, light pink, or dark purple. In the test performed with agarose gel as a model, the color of the test paper could be observed and recorded after 2 min, and the color significantly changed with increasing glucose concentration when this concentration exceeded 5.6 mM [25].

Colorimetry was also be used for uric acid detection. The reaction between uric acid in ISF and uricase embedded in poly(vinyl alcohol) microneedles generated H_2O_2, which reacted with 3,3′,5,5′-tetramethylbenzidine under the action of polypyridine nanoparticles wrapped in the display layer to induce a color change. Image analysis allowed the uric acid level to be accurately quantified within the range of 200–1000 μM, with the detection limit determined as ~65 μM [126].

To realize the simultaneous colorimetric detection of multiple substances in ISF, Zhu et al. [24] imprinted nitrocellulose membranes with wax to create hydrophobic boundaries delineating the detection areas for glucose, lactate, cholesterol, and H^+ and preventing the mixing of reagents used in different detection quadrants (Fig. 8C) [24]. The microneedles used with the test strips consisted of cross-linked methacrylic acid and soluble hyaluronic acid with an absorption capacity of 16.22 μL in 20 min.

Colorimetric analysis enables detection through visual inspection and is easy to implement, inexpensive, and color comparison-based. However, the subtle variations in color induced by slight concentration changes cannot be identified by the naked eye, and the concentration must reach a certain threshold before a color change appears. Although the realization of accurate quantitative colorimetric analysis still faces difficulties, this technique can be

combined with smartphones to enable red, green, and blue quantitative analysis.

The above microneedle-based systems interfaced with smartphones, lateral flow cassettes, and colorimetric phases are easy to use and suitable for long-term daily monitoring and management of patients with chronic diseases, and have commercial development value.

4.4. Closed-loop drug monitoring/delivery systems

Microneedles have been widely used in drug delivery, and the microneedle-based extraction of ISF for in vivo drug analysis and monitoring has significantly advanced over the years. Microneedles can serve as conduits for the exchange of substances both inside and outside the body. Therefore, a closed-loop microneedle-based system can be developed to automate real-time drug monitoring and delivery.

Hu et al. [27] developed a device integrating H_2O_2-responsive polymeric vesicles and a 20 × 20 array cross-linked hyaluronic acid microneedle patch. In this device, the polymeric vesicles were both a component of the glucose sensing element and an insulin release promoter. When the glucose level exceeded a certain value, insulin-loaded polymeric vesicles were released. A typical insulin-loaded microneedle brought blood glucose concentration to ~90 mg/dL within 1 h and maintained it in the normal range (<200 mg/dL) for ~5 h, but subsequently lost control, which resulted in a gradual increase in blood glucose level. This device mimicked the endocrine function of the pancreas, integrally monitoring glucose concentrations and releasing insulin to maintain relatively stable blood glucose levels. Later, researchers improved and supplemented the microneedle structure and the vesicle response principle to afford an "artificial pancreas" for the effective regulation of blood glucose levels [40,127,128].

Although this self-adjustable intelligent insulin administration device was only tested on animals (piglets and mice), it represents significant progress in the development of a closed-loop monitoring drug delivery system and opens up a new path for microneedle development.

5. Microneedle-based monitoring of plant metabolites

5.1. Extraction of plant metabolites for analysis

During their evolution, plants have developed many distinct metabolites, which are mostly found within single cells, provide protection from herbivores, and are usually the source of plant odor. Such metabolites can be researched to create more enticing foods, flavors, and perfumes [129,130]. Metabolites are often the chemical basis for the therapeutic action of medicinal plants and have been used to develop many medications [131]. With the development and use of concepts such as herbgenomics, metabolomics, and the potential economic worth of plant metabolites, this topic has been drawing increased attention [132,133].

Solid-liquid extraction, also known as maceration, is a traditional technique of plant metabolite extraction [134]. Recently, new extraction methods have been developed by combining auxiliary techniques, as exemplified by ultrasound-assisted extraction, microwave-assisted extraction, pressurized liquid extraction, and supercritical fluid extraction. The performance of these techniques depends on the employed solvent and physical parameters. Moreover, such techniques are more expensive than traditional ones.

The use of microneedles for drug administration and extraction has been thoroughly investigated in humans and animals, but not in plants. Flat comb-shaped microneedle arrays constructed on a silicon-on-insulator wafer (5 mm × 5 mm) were used to efficiently insert genome-editing proteins into plant tissues by carefully regulating the entry point. Notably, β-glucuronidase was expressed following microneedle insertion, and the direct delivery of the Cas9 ribonucleoprotein targeting the PDS11/18 gene resulted in the deletion of 11 bp at the locus in the branch meristematic tissues of soybeans [135].

As many plants are the source of herbal medicines, the analysis of their growth status and active ingredients is a matter of high practical significance. To extract pertinent compounds from stored plant metabolites, researchers have envisioned the usage of compact microneedles and performed some work in this direction.

5.1.1. Microneedle-based extraction of plant metabolites

Aluminosilicate microneedles and neural network-based image analysis were used to accurately identify metabolite-rich cells in rosemary and automatically extract compounds of interest from the same. The extraction efficacies of four different microneedle tip shapes (blunt narrow, blunt wide, beveled narrow, and beveled wide) were analyzed to maximize the amount of extracted metabolites and minimize the extraction time, reduce tissue injury, and overcome the viscous flow resistance of metabolic fluid [31]. Needles with beveled wide tips exhibited the best performance.

Compared to skilled manual activity, automated procedures are more efficient. Yet, manual control is relatively flexible, whereas the above extraction requires a reasonably flat leaf surface. However, the actual plant morphology is complicated and diverse, necessitating more advanced programming. Additionally, the microneedle size must be decreased to accommodate smaller plant cells, which puts more strain on the associated preparation process.

5.1.2. Microneedle-based in situ extraction of metabolites and diagnostic monitoring

Many plants are raw materials for Chinese medicinal materials, and pathogenic infections lead to crop failure. Ramos-Gómez et al. [136] realized the in situ molecular diagnosis of plant diseases by extracting and isolating pathogenic DNA from plant tissues for nucleic acid amplification. However, the standard method of phytoplasma DNA extraction employs cetyltrimethylammonium bromide and requires 3–4 h to isolate DNA by lysing tissues and cells, which is a cumbersome process (Fig. 9A) [29]. To circumvent this restriction, 15 × 15 poly(vinyl alcohol) microneedle arrays (needle length = 800 μm, base radius = 150 μm, tip radius = 5 μm) were created by vacuum micromolding. The microneedle patches punctured leaf tissues to break plant barriers (cell walls, epidermis, and the outer layer of the waxy cuticle) and thus enabled the isolation of DNA from insoluble plant tissues in <1 min (Fig. 9A). Paul et al. (Fig. 9B) [30] improved the initial procedure to include RNA and combined a microneedle patch with a 3D-printed smartphone imaging system to enable the immediate in-field detection of plant infections in <30 min. This approach facilitates the screening and analysis of plant diseases by farmers or extension agents during the planting process to ensure the high yield and quality of herbs.

Precision agriculture helps to increase the yield of herbs. Plant physiological states are reflected by changes in their ion content, membrane permeability, and viscosity. Electrical impedance spectroscopy can be used to rapidly and nondestructively examine these changes; however, this method is constrained by the plant barrier layer [137]. The combination of microneedles and an impedance measurement sensor overcomes this restriction, as microneedles can pass through the cuticle (Fig. 9C) [138]. Microneedles can penetrate the stratum corneum, and the combination of

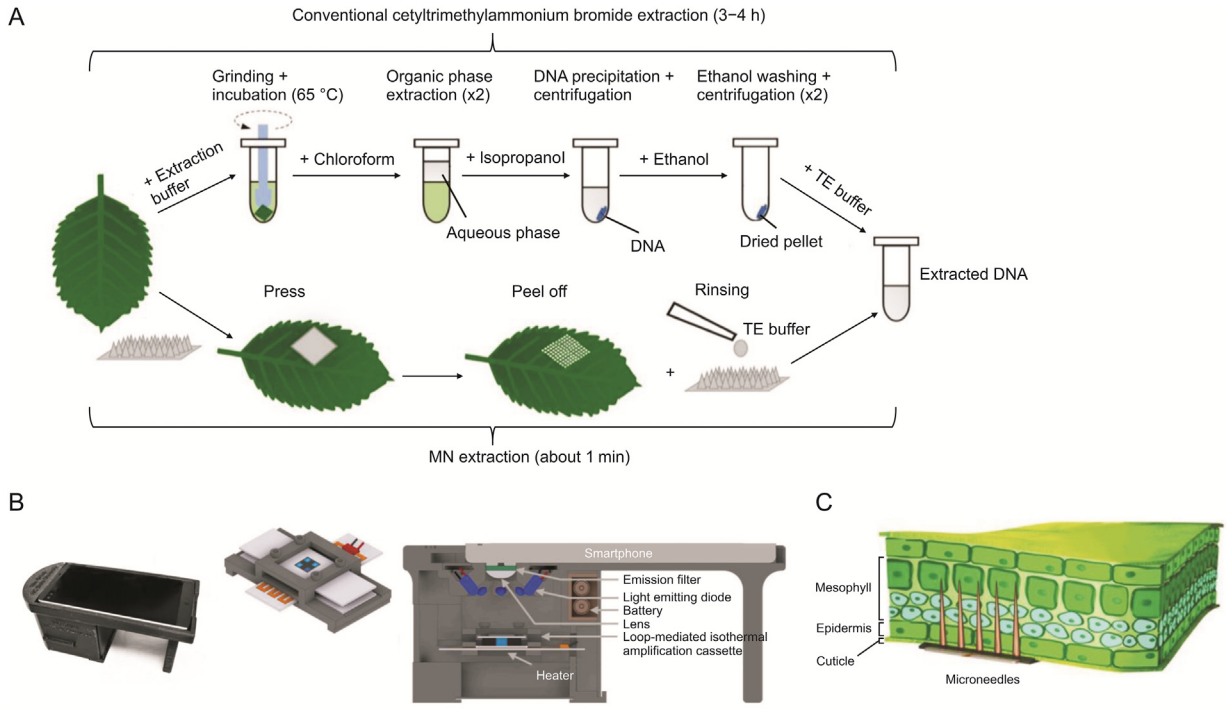

Fig. 9. Microneedle-based in situ extraction of metabolites and diagnostic monitoring. (A) Traditional (cetyltrimethylammonium bromide-based) and microneedle-based extraction of DNA from plant leaves [29]. (B) Microneedle-loop-mediated isothermal amplification platform-smartphone integrated device suitable for the in situ extraction and diagnosis of plant pathogens [30]. (C) Microneedle bioimpedance sensor acting on plant leaves [138]. TE: tris ethylenediaminetetraacetic acid. (Reprint from Refs. [29,30,138] with permission.)

microneedles with an impedance measuring sensor, where each microneedle in the microneedle array (10 × 10) is 350 μm long, overcomes this constraint. In an open-air setting, this system generated a more sensitive impedance spectrum with an average relative noise value of 3.83%, thus outperforming a standard planar sensor [138]. For the in situ detection of salicylic acid (SA, a plant hormone), a microneedle electrode created by microforming was paired with a sensor using molecularly imprinted polymers. After the microneedles pierced the cuticle, the imprinted polymers on the working electrode bound isolated SA and detected it through electro-oxidation (detection range = 5–150 μM, detection limit = 2.74 μM). The above apparatus could discriminate between basal SA levels in SA-deficient mutants and wild-type plants in an experiment performed with *Arabidopsis* leaves [139].

Additionally, when the external conditions governing growth, growing years, and harvesting time fluctuate, the contents of various compounds and active substances in Chinese herbal medicines change, and so do the related therapeutic effects [140]. For instance, yellow light encourages the growth and concentration of bioactive flavonoids in *Epimedium* [141], while the exposure of mulberry leaves to frost is thought to enhance their therapeutic effects [142]. High-performance liquid chromatography has been used to determine the contents of one or more components of Chinese herbal medicines. Although the sensitivity and efficiency of this method are growing, its widespread use remains constrained by the need for expensive equipment and stringent sample pretreatment procedures [143,144]. The problems posed by the low sampling amount and time-consuming nature of microneedle-based ISF extraction can be overcome by increasing the density of microneedle arrays. For example, a high density of 625 silicon microneedles per mm^2 in a single array was realized using dry etching [145]. The mass production of microneedles also faces some challenges such as elevated investment risk, lack of standard production methods, and the non-standardized evaluation of quality and sterility requirements during processing. Nevertheless, relevant regulatory work groups have been established to identify and address the problems of microneedle manufacturing [146].

The above microneedle-based plant metabolite extraction-detection devices help to understand the growth status of plants. The efficiency and portable nature of such devices enable in-field plant diagnostics and allow the state of the plant body to be determined without disturbing growth, thus facilitating in-field plant disease screening and analysis by farmers or extension workers. Future works should deal with the combination of microneedles with various sensors and machinery to enable automated extraction and the in situ monitoring of the plant body state. Currently, this area is insufficiently researched, and the related development is hindered by challenges associated with the accurate identification of specific cells containing metabolites, the differentiation of cell types, and the design of more suitable microneedles for the smooth penetration of and removal from sticky plant tissues.

6. Conclusions and future perspectives

Since it was first proposed, the usage of microneedles has drawn much attention and experienced rapid development. Currently, microneedles find applications not only in cosmetic and delivery therapies, but also in medication analysis and monitoring; although, much progress remains to be made in the latter field.

Some works used microneedles to extract pharmaceuticals or biomarkers from ISF and then performed sophisticated analysis using various methods and devices. As a result, technologies combining microneedles and sensors for in situ extraction and monitoring have emerged. In the context of the COVID-19 pandemic, the combination of microneedles with sensors, smartphones, and lateral flow boxes makes it easier for patients with chronic diseases to test themselves at home, optimizes therapy by keeping track of the results, and satisfies people's increased aspirations for better health.

In view of the ex vivo nature of such analysis, the damage inflicted by the sampling procedure is irreversible, and for many uncommon and precious herbal medications, the cost is high. The combination of microneedling with smartphones and other applications in the study of herbal medicines facilitates the in-field diagnosis of growth conditions and the evaluation of the active ingredients of plants with minimal damage. Future applications of microneedles include the monitoring of herb active ingredients, disease diagnosis and treatment, and the identification of optimal growth conditions. This microneedle-based monitoring has significant practical implications for the creation, assessment, and quality control of traditional Chinese medicines.

The microneedle-based extraction of ISF for drug monitoring and analysis has promising future applications. For example, microneedles should be more closely integrated with smartphones, sensors, etc. The development of closed-loop extraction-sensing-monitoring-delivery systems based on microneedles will facilitate the analysis of medications, biomarkers, metabolites, and other substances and thus make it easier to diagnose and treat patients as well as assess the efficacy of herbs.

Currently, the microneedle-based extraction of ISF for drug analysis faces certain difficulties, which, however, are not insurmountable. In addition, some problems will be solved over time with increasing research depth. For example, sensors specific to different drugs or biomarkers have to be developed based on their properties; the structure of human skin differs from that of animal skin, and microneedle patches successfully tested in animal models need more relevant clinical trials. Moreover, only few types of drugs have been studied and successfully tested. These efforts in mass production and experimental design are expected to provide a solid foundation for the broad application of microneedle-based drug analysis.

CRediT author statement

Shuwen Ma: Conceptualization, Methodology, Writing - Original draft preparation, Software; **Jiaqi Li:** Software, Writing - Reviewing and Editing, Formal analysis; **Lixia Pei:** Visualization, Data curation, Writing - Reviewing and Editing; **Nianping Feng:** Methodology, Supervision, Resources; **Yongtai Zhang:** Supervision, Project administration, Funding acquisition, Writing - Reviewing and Editing.

Declaration of competing interest

The authors declare that there are no conflicts of interest.

Acknowledgments

This work was financially supported by the National Natural Science Foundation of China (Grant No.: 82074031), the Program for Professor of Special Appointment (Eastern Scholar) at Shanghai Institutions of Higher Learning (Grant No.: TP2020054), China, and Program for Shanghai High-level Local University Innovation Team (Grant No.: SZY20220315), China.

References

[1] A.H. Gershlick, Y.D. Syndercombe Court, A.J. Murday, et al., Adverse effects of high dose aspirin on platelet adhesion to experimental autogenous vein grafts, Cardiovasc. Res. 19 (1985) 770–776.
[2] H. Carlsson, K. Hjorton, S. Abujrais, et al., Measurement of hydroxychloroquine in blood from SLE patients using LC-HRMS-evaluation of whole blood, plasma, and serum as sample matrices, Arthritis Res. Ther. 22 (2020), 125.
[3] A. Siddiqi, D.A. Khan, F.A. Khan, et al., Therapeutic drug monitoring of amikacin in preterm and term infants, Singapore Med. J. 50 (2009) 486–489.
[4] C. Domes, R. Domes, J. Popp, et al., Ultrasensitive detection of antiseptic antibiotics in aqueous media and human urine using deep UV resonance Raman spectroscopy, Anal. Chem. 89 (2017) 9997–10003.
[5] V. Franco, G. Gatti, I. Mazzucchelli, et al., Relationship between saliva and plasma rufinamide concentrations in patients with epilepsy, Epilepsia 61 (2020) e79–e84.
[6] M. Nakajima, S. Sato, S. Yamato, et al., Assessment of tear concentrations on therapeutic drug monitoring. III. Determination of theophylline in tears by gas chromatography/mass spectrometry with electron ionization mode, Drug Metabol. Pharmacokinet. 18 (2003) 139–145.
[7] K. Rebrin, G.M. Steil, Can interstitial glucose assessment replace blood glucose measurements? Diabetes Technol. Ther. 2 (2000) 461–472.
[8] T. Altendorfer-Kroath, D. Schimek, A. Eberl, et al., Comparison of cerebral Open Flow Microperfusion and Microdialysis when sampling small lipophilic and small hydrophilic substances, J. Neurosci. Methods 311 (2019) 394–401.
[9] J.D. Ulrich, J.M. Burchett, J.L. Restivo, et al., *In vivo* measurement of apolipoprotein E from the brain interstitial fluid using microdialysis, Mol. Neurodegener. 8 (2013), 13.
[10] J. Wen, X. Chen, Y. Yang, et al., Acupuncture medical therapy and its underlying mechanisms: A systematic review, Am. J. Chin. Med. 49 (2021) 1–23.
[11] X. Wang, Y. Han, J. Jin, et al., Plum-blossom needle assisted photodynamic therapy for the treatment of oral potentially malignant disorder in the elderly, Photodiagnosis Photodyn. Ther. 25 (2019) 296–299.
[12] K. Cheung, D.B. Das, Microneedles for drug delivery: Trends and progress, Drug Deliv. 23 (2016) 2338–2354.
[13] S. Henry, D.V. McAllister, M.G. Allen, et al., Microfabricated microneedles: A novel approach to transdermal drug delivery, J. Pharm. Sci. 87 (1998) 922–925.
[14] S.A.N. Gowers, D.M.E. Freeman, T.M. Rawson, et al., Development of a minimally invasive microneedle-based sensor for continuous monitoring of β-lactam antibiotic concentrations *in vivo*, ACS Sens. 4 (2019) 1072–1080.
[15] S. Samavat, J. Lloyd, L. O'Dea, et al., Uniform sensing layer of immiscible enzyme-mediator compounds developed via a spray aerosol mixing technique towards low cost minimally invasive microneedle continuous glucose monitoring devices, Biosens. Bioelectron. 118 (2018) 224–230.
[16] J. Gupta, S.S. Park, B. Bondy, et al., Infusion pressure and pain during microneedle injection into skin of human subjects, Biomaterials 32 (2011) 6823–6831.
[17] M. Li, L.K. Vora, K. Peng, et al., Trilayer microneedle array assisted transdermal and intradermal delivery of dexamethasone, Int. J. Pharm. 612 (2022), 121295.
[18] Z. Wang, J. Luan, A. Seth, et al., Microneedle patch for the ultrasensitive quantification of protein biomarkers in interstitial fluid, Nat. Biomed. Eng. 5 (2021) 64–76.
[19] P.M. Wang, M. Cornwell, M.R. Prausnitz, Minimally invasive extraction of dermal interstitial fluid for glucose monitoring using microneedles, Diabetes Technol. Therapeut. 7 (2005) 131–141.
[20] L. Bao, J. Park, B. Qin, et al., Anti-SARS-CoV-2 IgM/IgG antibodies detection using a patch sensor containing porous microneedles and a paper-based immunoassay, Sci. Rep. 12 (2022), 10693.
[21] Y. Zheng, R. Omar, R. Zhang, et al., A wearable microneedle-based extended gate transistor for real-time detection of sodium in interstitial fluids, Adv. Mater. 34 (2022), e2108607.
[22] H. Teymourian, C. Moonla, F. Tehrani, et al., Microneedle-based detection of ketone bodies along with glucose and lactate: Toward real-time continuous interstitial fluid monitoring of diabetic ketosis and ketoacidosis, Anal. Chem. 92 (2020) 2291–2300.
[23] P. Joshi, P.R. Riley, R. Mishra, et al., Transdermal polymeric microneedle sensing platform for fentanyl detection in biofluid, Biosensors (Basel) 12 (2022), 198.
[24] D.D. Zhu, L.W. Zheng, P.K. Duong, et al., Colorimetric microneedle patches for multiplexed transdermal detection of metabolites, Biosens. Bioelectron. 212 (2022), 114412.
[25] T. Wu, X. You, Z. Chen, Hollow microneedles on a paper fabricated by standard photolithography for the screening test of prediabetes, Sensors (Basel) 22 (2022), 4253.
[26] Y.J. Chen, Y.P. Hsu, Y.L. Tain, et al., Microneedle patches integrated with lateral flow cassettes for blood-free chronic kidney disease point-of-care testing during a pandemic, Biosens. Bioelectron. 208 (2022), 114234.
[27] X. Hu, J. Yu, C. Qian, et al., H_2O_2-responsive vesicles integrated with transcutaneous patches for glucose-mediated insulin delivery, ACS Nano 11 (2017) 613–620.
[28] H. Teymourian, M. Parrilla, J.R. Sempionatto, et al., Wearable electrochemical sensors for the monitoring and screening of drugs, ACS Sens. 5 (2020) 2679–2700.
[29] R. Paul, A.C. Saville, J.C. Hansel, et al., Extraction of plant DNA by microneedle patch for rapid detection of plant diseases, ACS Nano 13 (2019) 6540–6549.
[30] R. Paul, E. Ostermann, Y. Chen, et al., Integrated microneedle-smartphone nucleic acid amplification platform for in-field diagnosis of plant diseases, Biosens. Bioelectron. 187 (2021), 113312.
[31] H. Bae, M. Paludan, J. Knoblauch, et al., Neural networks and robotic microneedles enable autonomous extraction of plant metabolites, Plant

Physiol. 186 (2021) 1435–1441.
[32] M. Guo, Y. Wang, B. Gao, et al., Shark tooth-inspired microneedle dressing for intelligent wound management, ACS Nano 15 (2021) 15316–15327.
[33] B. Szeto, A. Aksit, C. Valentini, et al., Novel 3D-printed hollow microneedles facilitate safe, reliable, and informative sampling of perilymph from guinea pigs, Hear. Res. 400 (2021), 108141.
[34] U. Detamornrat, E. McAlister, A.R.J. Hutton, et al., The role of 3D printing technology in microengineering of microneedles, Small 18 (2022), e2106392.
[35] S. Choo, S. Jin, J. Jung, Fabricating high-resolution and high-dimensional microneedle mold through the resolution improvement of stereolithography 3D printing, Pharmaceutics 14 (2022), 766.
[36] C.J.W. Bolton, O. Howells, G.J. Blayney, et al., Hollow silicon microneedle fabrication using advanced plasma etch technologies for applications in transdermal drug delivery, Lab Chip 20 (2020) 2788–2795.
[37] E.M. Cahill, S. Keaveney, V. Stuettgen, et al., Metallic microneedles with interconnected porosity: A scalable platform for biosensing and drug delivery, Acta Biomater. 80 (2018) 401–411.
[38] G. Du, P. He, J. Zhao, et al., Polymeric microneedle-mediated transdermal delivery of melittin for rheumatoid arthritis treatment, J. Control. Release 336 (2021) 537–548.
[39] P. Liu, H. Du, Z. Wu, et al., Hydrophilic and anti-adhesive modification of porous polymer microneedles for rapid dermal interstitial fluid extraction, J. Mater. Chem. B 9 (2021) 5476–5483.
[40] J. Wang, Y. Ye, J. Yu, et al., Core-shell microneedle gel for self-regulated insulin delivery, ACS Nano 12 (2018) 2466–2473.
[41] T. Sato, S. Okada, K. Hagino, et al., Measurement of glucose area under the curve using minimally invasive interstitial fluid extraction technology: Evaluation of glucose monitoring concepts without blood sampling, Diabetes Technol. Ther. 13 (2011) 1194–1200.
[42] P.R. Miller, R.M. Taylor, B.Q. Tran, et al., Extraction and biomolecular analysis of dermal interstitial fluid collected with hollow microneedles, Commun. Biol. 1 (2018), 173.
[43] Y. Chen, B.Z. Chen, Q.L. Wang, et al., Fabrication of coated polymer microneedles for transdermal drug delivery, J. Control. Release 265 (2017) 14–21.
[44] E. Caffarel-Salvador, A.J. Brady, E. Eltayib, et al., Hydrogel-forming microneedle arrays allow detection of drugs and glucose *in vivo*: Potential for use in diagnosis and therapeutic drug monitoring, PLoS One 10 (2015), e0145644.
[45] Z. Li, Y. He, L. Deng, et al., A fast-dissolving microneedle array loaded with chitosan nanoparticles to evoke systemic immune responses in mice, J. Mater. Chem. B 8 (2020) 216–225.
[46] W. Zhu, S. Li, C. Wang, et al., Enhanced immune responses conferring cross-protection by skin vaccination with a tri-component influenza vaccine using a microneedle patch, Front. Immunol. 9 (2018), 1705.
[47] C. Caudill, J.L. Perry, K. Iliadis, et al., Transdermal vaccination via 3D-printed microneedles induces potent humoral and cellular immunity, Proc. Natl. Acad. Sci. U S A 118 (2021), e2102595118.
[48] J. Yu, C. Kuwentrai, H.R. Gong, et al., Intradermal delivery of mRNA using cryomicroneedles, Acta Biomater. 148 (2022) 133–141.
[49] Y. Hu, Y. Mo, J. Wei, et al., Programmable and monitorable intradermal vaccine delivery using ultrasound perforation array, Int. J. Pharm. 617 (2022), 121595.
[50] Y. Lee, T. Kang, H.-R. Cho, et al., Localized delivery of theranostic nanoparticles and high-energy photons using microneedles-on-bioelectronics, Adv. Mater. 33 (2021), e2100425.
[51] H. Chang, S.W.T. Chew, M. Zheng, et al., Cryomicroneedles for transdermal cell delivery, Nat. Biomed. Eng. 5 (2021) 1008–1018.
[52] A. Abramson, E. Caffarel-Salvador, V. Soares, et al., A luminal unfolding microneedle injector for oral delivery of macromolecules, Nat. Med. 25 (2019) 1512–1518.
[53] J. Tang, J. Wang, K. Huang, et al., Cardiac cell-integrated microneedle patch for treating myocardial infarction, Sci. Adv. 4 (2018), eaat9365.
[54] E. Caffarel-Salvador, S. Kim, V. Soares, et al., A microneedle platform for buccal macromolecule delivery, Sci. Adv. 7 (2021), eabe2620.
[55] M. Cui, M. Zheng, C. Wiraja, et al., Ocular delivery of predatory bacteria with cryomicroneedles against eye infection, Adv. Sci. 8 (2021), e2102327.
[56] J.J. Chae, J.H. Jung, W. Zhu, et al., Drug-free, nonsurgical reduction of intraocular pressure for four months after suprachoroidal injection of hyaluronic acid hydrogel, Adv. Sci. (Weinh) 8 (2021), 2001908.
[57] H. Shi, J. Zhou, Y. Wang, et al., A rapid corneal healing microneedle for efficient ocular drug delivery, Small 18 (2022), e2104657.
[58] G. Roy, P. Garg, V.V.K. Venuganti, Microneedle scleral patch for minimally invasive delivery of triamcinolone to the posterior segment of eye, Int. J. Pharm. 612 (2022), 121305.
[59] J. Lee, D.-H. Kim, K.J. Lee, et al., Transfer-molded wrappable microneedle meshes for perivascular drug delivery, J. Control. Release 268 (2017) 237–246.
[60] Y. Liu, L. Long, F. Zhang, et al., Microneedle-mediated vascular endothelial growth factor delivery promotes angiogenesis and functional recovery after stroke, J. Control. Release 338 (2021) 610–622.
[61] Z. Wang, Z. Yang, J. Jiang, et al., Silk microneedle patch capable of on-demand multidrug delivery to the brain for glioblastoma treatment, Adv. Mater. 34 (2022), e2106606.
[62] D. Jakka, A.V. Matadh, H.N. Shivakumar, et al., Polymer Coated Polymeric (PCP) microneedles for sampling of drugs and biomarkers from tissues, Eur. J. Pharmaceut. Sci. 175 (2022), 106203.
[63] F. Liu, Z. Lin, Q. Jin, et al., Protection of nanostructures-integrated microneedle biosensor using dissolvable polymer coating, ACS Appl. Mater. Interfaces 11 (2019) 4809–4819.
[64] Y. Ito, M. Taniguchi, A. Hayashi, et al., Application of dissolving microneedles to glucose monitoring through dermal interstitial fluid, Biol. Pharm. Bull. 37 (2014) 1776–1781.
[65] Y. Ito, Y. Inagaki, S. Kobuchi, et al., Therapeutic drug monitoring of vancomycin in dermal interstitial fluid using dissolving microneedles, Int. J. Med. Sci. 13 (2016) 271–276.
[66] R. He, Y. Niu, Z. Li, et al., A hydrogel microneedle patch for point-of-care testing based on skin interstitial fluid, Adv. Healthc. Mater. 9 (2020), e1901201.
[67] A.M. Tsimberidou, E. Fountzilas, M. Nikanjam, et al., Review of precision cancer medicine: Evolution of the treatment paradigm, Cancer Treat Rev. 86 (2020), 102019.
[68] S. Dhaese, S. Van Vooren, J. Boelens, et al., Therapeutic drug monitoring of β-lactam antibiotics in the ICU, Expert Rev. Anti Infect. Ther. 18 (2020) 1155–1164.
[69] I. Aícua-Rapún, P. André, A.O. Rossetti, et al., Therapeutic drug monitoring of newer antiepileptic drugs: A randomized trial for dosage adjustment, Ann. Neurol. 87 (2020) 22–29.
[70] S.W. Syversen, K.K. Jørgensen, G.L. Goll, et al., Effect of therapeutic drug monitoring vs standard therapy during maintenance infliximab therapy on disease control in patients with immune-mediated inflammatory diseases: A randomized clinical trial, JAMA 326 (2021) 2375–2384.
[71] K. Papamichael, A.S. Cheifetz, G.Y. Melmed, et al., Appropriate therapeutic drug monitoring of biologic agents for patients with inflammatory bowel diseases, Clin. Gastroenterol. Hepatol. 17 (2019) 1655–1668.e3.
[72] R. Simeoli, T.P.C. Dorlo, L.M. Hanff, et al., Editorial: Therapeutic drug monitoring (TDM): A useful tool for pediatric pharmacology applied to routine clinical practice, Front. Pharmacol. 13 (2022), 931843.
[73] G. Özalp Gerçeker, D. Ayar, E.Z. Özdemir, et al., Effects of virtual reality on pain, fear and anxiety during blood draw in children aged 5–12 years old: A randomised controlled study, J. Clin. Nurs. 29 (2020) 1151–1161.
[74] M. Hoelscher, G. Riedner, Y. Hemed, et al., Estimating the number of HIV transmissions through reused syringes and needles in the Mbeya Region, Tanzania, AIDS 8 (1994) 1609–1615.
[75] J. Hauser, G. Lenk, J. Hansson, et al., High-yield passive plasma filtration from human finger prick blood, Anal. Chem. 90 (2018) 13393–13399.
[76] Blood-Clotting, Lancet 1 (1953) 834–836.
[77] H. Hjelmgren, A. Nilsson, I.H. Myrberg, et al., Capillary blood sampling increases the risk of preanalytical errors in pediatric hospital care: Observational clinical study, J. Spec. Pediatr. Nurs. 26 (2021), e12337.
[78] Y. Kim, M.R. Prausnitz, Sensitive sensing of biomarkers in interstitial fluid, Nat. Biomed. Eng. 5 (2021) 3–5.
[79] Y. Nisimaru, The basis of angiology. A concept of body fluid circulation, Hiroshima J. Med. Sci. 24 (1975) 1–58.
[80] K.L. Skorecki, B.M. Brenner, Body fluid homeostasis in man: A contemporary overview, Am. J. Med. 70 (1981) 77–88.
[81] L.L. Hill, Body composition, normal electrolyte concentrations, and the maintenance of normal volume, tonicity, and acid-base metabolism, Pediatr. Clin. North Am. 37 (1990) 241–256.
[82] M.M. Niedzwiecki, P. Samant, D.I. Walker, et al., Human suction blister fluid composition determined using high-resolution metabolomics, Anal. Chem. 90 (2018) 3786–3792.
[83] N.K. Gibbs, M. Norval, Urocanic acid in the skin: A mixed blessing? J. Invest. Dermatol. 131 (2011) 14–17.
[84] N. Minois, Molecular basis of the 'anti-aging' effect of spermidine and other natural polyamines - a mini-review, Gerontology 60 (2014) 319–326.
[85] S. Pajares, A. Arias, J. García-Villoria, et al., Role of creatine as biomarker of mitochondrial diseases, Mol. Genet. Metabol. 108 (2013) 119–124.
[86] G. Kugler, Myocardial release of lactate, inosine and hypoxanthine during atrial pacing and exercise-induced angina, Circulation 59 (1979) 43–49.
[87] M.T. Grinde, N. Skrbo, S.A. Moestue, et al., Interplay of choline metabolites and genes in patient-derived breast cancer xenografts, Breast Cancer Res. 16 (2014), R5.
[88] T. Shibata, F. Nakashima, K. Honda, et al., Toll-like receptors as a target of food-derived anti-inflammatory compounds, J. Biol. Chem. 289 (2014) 32757–32772.
[89] T.K.L. Kiang, V. Schmitt, M.H.H. Ensom, et al., Therapeutic drug monitoring in interstitial fluid: A feasibility study using a comprehensive panel of drugs, J. Pharm. Sci. 101 (2012) 4642–4652.
[90] S. Ullah, F. Hamade, U. Bubniene, et al., *In-vitro* model for assessing glucose diffusion through skin, Biosens. Bioelectron. 110 (2018) 175–179.
[91] A.K. Nilsson, U. Sjöbom, K. Christenson, et al., Lipid profiling of suction blister fluid: Comparison of lipids in interstitial fluid and plasma, Lipids Health Dis. 18 (2019), 164.
[92] E. Fryk, J.P. Sundelin, L. Strindberg, et al., Microdialysis and proteomics of subcutaneous interstitial fluid reveals increased galectin-1 in type 2 diabetes patients, Metabolism 65 (2016) 998–1006.
[93] S. Schroepf, D. Burau, H.-G. Muench, et al., Microdialysis sampling to monitor target-site vancomycin concentrations in septic infants: A feasible way to

close the knowledge gap, Int. J. Antimicrob. Agents 58 (2021), 106405.
[94] T.S. Anbar, N.H. Moftah, M.A.M. El-Khayyat, et al., Syringes versus Chinese cups in harvesting suction-induced blister graft: A randomized split-body study, Int. J. Dermatol. 57 (2018) 1249–1252.
[95] T.B. Rojahn, V. Vorstandlechner, T. Krausgruber, et al., Single-cell transcriptomics combined with interstitial fluid proteomics defines cell type-specific immune regulation in atopic dermatitis, J. Allergy Clin. Immunol. 146 (2020) 1056–1069.
[96] J. Kool, L. Reubsaet, F. Wesseldijk, et al., Suction blister fluid as potential body fluid for biomarker proteins, Proteomics 7 (2007) 3638–3650.
[97] E. Larrañeta, M.T.C. McCrudden, A.J. Courtenay, et al., Microneedles: A new frontier in nanomedicine delivery, Pharm. Res. 33 (2016) 1055–1073.
[98] T. Lange, A. Thomas, K. Walpurgis, et al., Fully automated dried blood spot sample preparation enables the detection of lower molecular mass peptide and non-peptide doping agents by means of LC-HRMS, Anal. Bioanal. Chem. 412 (2020) 3765–3777.
[99] L.M. Strambini, A. Longo, S. Scarano, et al., Self-powered microneedle-based biosensors for pain-free high-accuracy measurement of glycaemia in interstitial fluid, Biosens. Bioelectron. 66 (2015) 162–168.
[100] M. Zheng, Z. Wang, H. Chang, et al., Osmosis-powered hydrogel microneedles for microliters of skin interstitial fluid extraction within minutes, Adv. Healthc. Mater. 9 (2020), e1901683.
[101] A.H.B. Sabri, Q.K. Anjani, R.F. Donnelly, Synthesis and characterization of sorbitol laced hydrogel-forming microneedles for therapeutic drug monitoring, Int. J. Pharm. 607 (2021), 121049.
[102] P.P. Samant, M.M. Niedzwiecki, N. Raviele, et al., Sampling interstitial fluid from human skin using a microneedle patch, Sci. Transl. Med. 12 (2020), eaaw0285.
[103] H. Chang, M. Zheng, X. Yu, et al., A swellable microneedle patch to rapidly extract skin interstitial fluid for timely metabolic analysis, Adv. Mater. 29 (2017), 1702243.
[104] J. Zhu, X. Zhou, H.J. Kim, et al., Gelatin methacryloyl microneedle patches for minimally invasive extraction of skin interstitial fluid, Small 16 (2020), e1905910.
[105] J. Chen, M. Wang, Y. Ye, et al., Fabrication of sponge-forming microneedle patch for rapidly sampling interstitial fluid for analysis, Biomed. Microdevices 21 (2019), 63.
[106] D.F.S. Fonseca, P.C. Costa, I.F. Almeida, et al., Swellable gelatin methacryloyl microneedles for extraction of interstitial skin fluid toward minimally invasive monitoring of urea, Macromol. Biosci. 20 (2020), e2000195.
[107] Y. Qiao, J. Du, R. Ge, et al., A sample and detection microneedle patch for psoriasis MicroRNA biomarker analysis in interstitial fluid, Anal. Chem. 94 (2022) 5538–5545.
[108] Y. Cai, S. Huang, Z. Zhang, et al., Bioinspired rotation microneedles for accurate transdermal positioning and ultraminimal-invasive biomarker detection with mechanical robustness, Research (Wash. D C) 2022 (2022), 9869734.
[109] C. Kolluru, M. Williams, J.S. Yeh, et al., Monitoring drug pharmacokinetics and immunologic biomarkers in dermal interstitial fluid using a microneedle patch, Biomed. Microdevices 21 (2019), 14.
[110] C. Kolluru, M. Williams, J. Chae, et al., Recruitment and collection of dermal interstitial fluid using a microneedle patch, Adv. Healthc. Mater. 8 (2019), e1801262.
[111] B.Q. Tran, P.R. Miller, R.M. Taylor, et al., Proteomic characterization of dermal interstitial fluid extracted using a novel microneedle-assisted technique, J. Proteome Res. 17 (2018) 479–485.
[112] T.M. Rawson, S.A.N. Gowers, D.M.E. Freeman, et al., Microneedle biosensors for real-time, minimally invasive drug monitoring of phenoxymethylpenicillin: A first-in-human evaluation in healthy volunteers, Lancet Digit. Health. 1 (2019) e335–e343.
[113] C. Tortolini, A.E.G. Cass, R. Pofi, et al., Microneedle-based nanoporous gold electrochemical sensor for real-time catecholamine detection, Mikrochim. Acta 189 (2022), 180.
[114] L. Fang, H. Ren, X. Mao, et al., Differential amperometric microneedle biosensor for wearable levodopa monitoring of Parkinson's disease, Biosensors (Basel) 12 (2022), 102.
[115] R.K. Mishra, K.Y. Goud, Z. Li, et al., Continuous opioid monitoring along with nerve agents on a wearable microneedle sensor array, J. Am. Chem. Soc. 142 (2020) 5991–5995.
[116] J. Ju, C.M. Hsieh, Y. Tian, et al., Surface enhanced Raman spectroscopy based biosensor with a microneedle array for minimally invasive *in vivo* glucose measurements, ACS Sens. 5 (2020) 1777–1785.
[117] M. Parrilla, U. Detamornrat, J. Domínguez-Robles, et al., Wearable hollow microneedle sensing patches for the transdermal electrochemical monitoring of glucose, Talanta 249 (2022), 123695.
[118] H.J. Kil, S.R. Kim, J.W. Park, A self-charging supercapacitor for a patch-type glucose sensor, ACS Appl. Mater. Interfaces 14 (2022) 3838–3848.
[119] P. Bollella, S. Sharma, A.E.G. Cass, et al., Microneedle-based biosensor for minimally-invasive lactate detection, Biosens. Bioelectron. 123 (2019) 152–159.
[120] A.M.V. Mohan, J.R. Windmiller, R.K. Mishra, et al., Continuous minimally-invasive alcohol monitoring using microneedle sensor arrays, Biosens. Bioelectron. 91 (2017) 574–579.
[121] B. Yang, J. Kong, X. Fang, Programmable CRISPR-Cas9 microneedle patch for long-term capture and real-time monitoring of universal cell-free DNA, Nat. Commun. 13 (2022), 3999.
[122] M. Parrilla, M. Cuartero, S. Padrell Sánchez, et al., Wearable all-solid-state potentiometric microneedle patch for intradermal potassium detection, Anal. Chem. 91 (2019) 1578–1586.
[123] Q. Li, R. Xu, H. Fan, et al., Smart mushroom-inspired imprintable and lightly detachable (MILD) microneedle patterns for effective COVID-19 vaccination and decentralized information storage, ACS Nano 16 (2022) 7512–7524.
[124] D. Poirier, F. Renaud, V. Dewar, et al., Hepatitis B surface antigen incorporated in dissolvable microneedle array patch is antigenic and thermostable, Biomaterials 145 (2017) 256–265.
[125] Y. Cheng, X. Gong, J. Yang, et al., A touch-actuated glucose sensor fully integrated with microneedle array and reverse iontophoresis for diabetes monitoring, Biosens. Bioelectron. 203 (2022), 114026.
[126] P. Zhang, X. Wu, H. Xue, et al., Wearable transdermal colorimetric microneedle patch for Uric acid monitoring based on peroxidase-like polypyrrole nanoparticles, Anal. Chim. Acta 1212 (2022), 339911.
[127] J. Wang, J. Yu, Y. Zhang, et al., Charge-switchable polymeric complex for glucose-responsive insulin delivery in mice and pigs, Sci. Adv. 5 (2019), eaaw4357.
[128] J. Yu, J. Wang, Y. Zhang, et al., Glucose-responsive insulin patch for the regulation of blood glucose in mice and minipigs, Nat. Biomed. Eng. 4 (2020) 499–506.
[129] J. Li, H. Hu, J. Mao, et al., Defense of pyrethrum flowers: Repelling herbivores and recruiting carnivores by producing aphid alarm pheromone, New Phytol. 223 (2019) 1607–1620.
[130] S. Xu, X. Zeng, H. Wu, et al., Characterizing volatile metabolites in raw Pu'er tea stored in wet-hot or dry-cold environments by performing metabolomic analysis and using the molecular sensory science approach, Food Chem. 350 (2021), 129186.
[131] G. Porras, F. Chassagne, J.T. Lyles, et al., Ethnobotany and the role of plant natural products in antibiotic drug discovery, Chem. Rev. 121 (2021) 3495–3560.
[132] T. Xin, Y. Zhang, X. Pu, et al., Trends in herbgenomics, Sci. China Life Sci. 62 (2019) 288–308.
[133] D. Li, E. Gaquerel, Next-generation mass spectrometry metabolomics revives the functional analysis of plant metabolic diversity, Annu. Rev. Plant Biol. 72 (2021) 867–891.
[134] M.E. Hergueta-Castillo, E. López-Rodríguez, R. López-Ruiz, et al., Targeted and untargeted analysis of triazole fungicides and their metabolites in fruits and vegetables by UHPLC-orbitrap-MS^2, Food Chem. 368 (2022), 130860.
[135] A. Viswan, A. Yamagishi, M. Hoshi, et al., Microneedle array-assisted, direct delivery of genome-editing proteins into plant tissue, Front. Plant Sci. 13 (2022), 878059.
[136] S. Ramos-Gómez, M.D. Busto, M. Perez-Mateos, et al., Development of a method to recovery and amplification DNA by real-time PCR from commercial vegetable oils, Food Chem. 158 (2014) 374–383.
[137] L. Chen, Z. Han, X. Fan, et al., An impedance-coupled microfluidic device for single-cell analysis of primary cell wall regeneration, Biosens. Bioelectron. 165 (2020), 112374.
[138] A. Bukhamsin, K. Moussi, R. Tao, et al., Robust, long-term, and exceptionally sensitive microneedle-based bioimpedance sensor for precision farming, Adv. Sci. (Weinh) 8 (2021), e2101261.
[139] A. Bukhamsin, A. Ait Lahcen, J.O. Filho, et al., Minimally-invasive, real-time, non-destructive, species-independent phytohormone biosensor for precision farming, Biosens. Bioelectron. 214 (2022), 114515.
[140] C. Bai, J. Yang, B. Cao, et al., Growth years and post-harvest processing methods have critical roles on the contents of medicinal active ingredients of medicinal active ingredients of *Scutellaria baicalensis*, Ind. Crop. Prod. 158 (2020), 112985.
[141] D.Q. Xu, S.Y. Cheng, J.Q. Zhang, et al., *Morus alba* L. Leaves - integration of their transcriptome and metabolomics dataset: Investigating potential genes involved in flavonoid biosynthesis at different harvest times, Front. Plant Sci. 12 (2021), 736332.
[142] Q. Yang, J. Pan, G. Shen, et al., Yellow ligaht promotes the growth and accumulation of bioactive flavonoids in *Epimedium pseudowushanense*, J. Photochem. Photobiol. B 197 (2019), 111550.
[143] J. Geng, L. Xiao, C. Chen, et al., An integrated analytical approach based on enhanced fragment ions interrogation and modified Kendrick mass defect filter data mining for in-depth chemical profiling of glucosinolates by ultra-high-pressure liquid chromatography coupled with Orbitrap high resolution mass spectrometry, J. Chromatogr. A 1639 (2021), 461903.
[144] X. He, S. Huang, M. Wu, et al., Simultaneous quantitative analysis of ten bioactive flavonoids in Citri Reticulatae Pericarpium Viride (Qing Pi) by ultrahigh-performance liquid chromatography and high-resolution mass spectrometry combined with chemometric methods, Phytochem. Anal. 32 (2021) 1152–1161.
[145] H. Roh, Y.J. Yoon, J.S. Park, et al., Fabrication of high-density out-of-plane microneedle arrays with various heights and diverse cross-sectional shapes, Nanomicro. Lett. 14 (2021), 24.
[146] B. Creelman, C. Frivold, S. Jessup, et al., Manufacturing readiness assessment for evaluation of the microneedle array patch industry: An exploration of barriers to full-scale manufacturing, Drug Deliv. Transl. Res. 12 (2022) 368–375.